AN EXPERIMENTAL INVESTIGATION OF POSSIBLE PRODUCTION MECHANISMS OF HYDRATE FORMATION

A THESIS SUBMITTED TO
THE GRADUATE SCHOOL OF NATURAL AND APPLIED SCIENCES
OF
MIDDLE EAST TECHNICAL UNIVERSITY

BY

HASAN HÜSEYİN ENGÜÇLÜ

IN PARTIAL FULFILLMENT OF THE REQUIREMENTS
FOR
THE DEGREE OF MASTER OF SCIENCE
IN
PETROLEUM AND NATURAL GAS ENGINEERING

SEPTEMBER 2021

Approval of the thesis:

AN EXPERIMENTAL INVESTIGATION OF POSSIBLE PRODUCTION MECHANISMS OF HYDRATE FORMATION

submitted by **HASAN HÜSEYİN ENGÜÇLÜ** in partial fulfillment of the requirements for the degree of **Master of Science** i**n Petroleum and Natural Gas Engineering, Middle East Technical University** by,

Prof. Dr. Halil Kalıpçılar
Dean, Graduate School of **Natural and Applied Sciences** _____

Assoc. Prof. Dr. Çağlar Sınayuç
Head of the Department, **Petroleum and Natural Gas Eng.** _____

Prof. Dr. Mahmut Parlaktuna
Supervisor, **Petroleum and Natural Gas Eng., METU** _____

Examining Committee Members:

Assoc. Prof. Dr. Çağlar Sınayuç
Petroleum and Natural Gas Eng., METU _____

Prof. Dr. Mahmut Parlaktuna
Petroleum and Natural Gas Eng., METU _____

Assist. Prof. Dr. Doruk Alp
Petroleum and Natural Gas Eng., METU - NCC _____

Date: 10.09.2021

I hereby declare that all information in this document has been obtained and presented in accordance with academic rules and ethical conduct. I also declare that, as required by these rules and conduct, I have fully cited and referenced all material and results that are not original to this work.

Name, Surname : Hasan Hüseyin Engüçlü

Signature :

ABSTRACT

AN EXPERIMENTAL INVESTIGATION OF POSSIBLE PRODUCTION MECHANISMS OF HYDRATE FORMATION

Engüçlü, Hasan Hüseyin
Master of Science, Petroleum and Natural Gas Engineering
Supervisor: Prof. Dr. Mahmut Parlaktuna

September 2021, 67 pages

In this study, temperature, pressure and mole values of methane hydrate formation and dissociation are analyzed using different production methods under laboratory conditions. During the experiments, a cylindrical high-pressure hydrate cell in a constant temperature room was used. In order to provide the real field conditions of the hydrate reservoirs, methane gas was injected at high pressure into the cell filled with sand and water at low temperatures, and the hydrate reservoir was formed in a 21.2 *liter hydrate formation cell by providing necessary thermodynamic conditions. A ¼ inch production line was used for production of methane and water in 3 different experiments. Production phase of the first two experiments were not discussed due to discrepancies arising from the production data. Two different production stages were applied in the third experiment. The first stage was carried out by combination of pressure reduction and thermal recovery method by providing constant temperature water circulation through the spiral pipe inside the cell. The thermal recovery method's effect decreased and disappeared in the second stage. It left its place only to the depressurization method.

As a result of the endothermic dissociation process of the production stage, the heat taken from the environment caused pores to be clogged due to reformation of the hydrate. This slowed down the production and made it stop from time to time. Using the depressurization method with the thermal recovery method, hydrate production became more effective and the hydrate dissociation rate increased. Depressurization method alone became less effective and the rate of dissociation decreased.

Keywords: Gas Hydrate Formation, Gas Hydrate Dissociation, Gas Hydrate Production Mechanisms, Depressurization, Thermal Recovery

ÖZ

HİDRAT OLUŞUMUNUN OLASI ÜRETİM MEKANİZMALARININ DENEYSEL İNCELENMESİ

Engüçlü, Hasan Hüseyin
Yüksek Lisans, Petrol ve Doğal Gaz Mühendisliği
Tez Yöneticisi: Prof. Dr. Mahmut Parlaktuna

Eylül 2021, 67 sayfa

Bu çalışmada, metan hidrat oluşumu ve ayrışmasının sıcaklık, basınç ve mol değerleri, laboratuvar koşullarında farklı üretim yöntemleri kullanılarak analiz edilmiştir. Deneysel çalışmalar sırasında sabit sıcaklık odasındaki silindirik yüksek basınca dayanaklı hidrat hücresi kullanılmıştır.

Hidrat rezervuarlarının gerçek saha koşullarının sağlanması için düşük sıcaklıktaki kum ve su ile dolu hücreye yüksek basınçta metan gazı basılmış ve gerekli termodinamik koşulların sağlanması ile hidrat rezervuarı 21.2 litrelik hücre hacminde oluşturulmuştur. Oluşan hidratın üretimi için hidrat hücresinin bağlı olduğu 1/4 inç dış çapındaki sabit sıcaklık odasından dışarıya devam eden üretim hattındaki test düzeneği kullanılmıştır. İlk iki deneyin üretim aşaması, üretim verilerinden kaynaklanan farklılıklar nedeniyle tartışılmamıştır. Üçüncü deneyde ise iki farklı üretim aşaması uygulanmıştır. İlk aşama, hücre içindeki spiral boru vasıtasıyla sabit sıcaklıkta su sirkülasyonu sağlanarak basınç düşürme ve ısıl kurtarım yöntemleri beraber uygulanmıştır. İkinci aşamada ise ısıl kurtarım yönteminin etkisi azalmış ve ortadan kalkmıştır. Yerini sadece basınç düşümü yöntemine bırakmıştır.

Üretim aşamasının endotermik ayrışma süreci sonucunda ortamdan alınan ısı hidratın yeniden oluşumuna ve gözenekli yapıyı tıkamasına neden olmuştur. Bu, üretimi yavaşlatmış ve zaman zaman durmasına neden olmuştur. Isıl kurtarım yöntemi ile basınç düşürme yöntemi kullanılarak hidrat üretimi daha etkili hale gelmiş ve hidrat ayrışma hızı artmıştır. Basınç düşürme yöntemi tek başına daha az etkili hale gelmiş ve ayrışma hızı azalmıştır.

Anahtar Kelimeler: Gaz Hidrat Oluşumu, Gaz Hidrat Çözünmesi, Gaz Hidrat Üretim Mekanizmaları, Basınç Düşürümü, Isıl Kurtarım)

To my family

ACKNOWLEDGMENTS

The author of the thesis wishes to express his greatest gratitude to his Advisor & Supervisor Prof. Dr. Mahmut Parlaktuna for their guidance, advice, criticism, encouragements and insight throughout the research. Also many thanks for suggestions and comments to the Head of the Department of Petroleum and Natural Gas Engineering, Assoc. Prof. Dr. Çağlar Sınayuç and Assist. Prof. Dr. Doruk Alp. Moreover, Asst. Prof. Dr. İsmail Durgut's knowledge sharing and leading on to draw 3d graphs, Dr. Sevtaç Bülbül's contributions in usage of computer program and industrial computer, Rabia Tuğçe Özdemir's cooperation on Matlab codes are appreciated. The technical assistance of Mr. Murat Çalışkan, Mr. Naci Doğru and Mr. Özgür Çoban are acknowledged.

TABLE OF CONTENTS

ABSTRACT v

ÖZ vii

ACKNOWLEDGMENTS x

TABLE OF CONTENTS xi

LIST OF TABLES xiii

LIST OF FIGURES xiv

LIST OF ABBREVIATIONS xvii

CHAPTERS

1 INTRODUCTION 1

2 LITERATURE REVIEW 3

2.1 An unconventional natural gas resource: Natural gas hydrates 3

2.2 Natural gas hydrate structures and classes 4

2.3 Formation – dissociation of hydrate 7

2.4 Natural gas hydrate laboratory studies in porous environment 9

3 STATEMENT OF THE PROBLEM 19

4 EXPERIMENTAL SET-UP AND PROCEDURE 21

4.1 Experimental set-up 21

4.1.1 Constant temperature room 22

4.1.2 Ambient temperature room 28

4.2 Experimental procedure 32
4.2.1 General procedure for hydrate formation 33
4.2.2 General procedure for gas production 34
5 RESULTS & DISCUSSIONS 35
5.1 EXPERIMENT 1 35
5.2 EXPERIMENT 2 38
5.3 EXPERIMENT 3 40
6 CONCLUSION 49
REFERENCES 51
APPENDICES
A. Paraview 3-D layered drawings for the Experiment 55

LIST OF TABLES

TABLES

Table 4.1 Measurements of cylindrical high pressure hydrate cell..... 24

LIST OF FIGURES

FIGURES

Figure 2.1. Resource Triangle for Natural Gas (Holditch, 2006) 3
Figure 2.2. Gas hydrate structures (Sloan D and Koh CA, 2008) 5
Figure 2.3. Hydrate classes; (a) Class-1, (b) Class-2, (c) Class-3, (d) Class-4 (Lee et al., 2011). 6
Figure 2.4. Hydrate equilibrium curve of pure methane 8
Figure 2.5. Schematic diagram of LARS (Schicks et al., 2011) 12
Figure 2.6. Schematic diagram of experimental set-up (Xiong et al., 2012) 13
Figure 2.7. Schematic diagram of experimental set-up (Örs and Sınayuç, 2012) ... 15
Figure 4.1. Experimental set-up 22
Figure 4.2. Constant temperature room 23
Figure 4.3. Components situated in the constant temperature room 23
Figure 4.4. Cylindrical high pressure cell used for hydrate formation experiments 24
Figure 4.5. The sand filling the hydrate cell 25
Figure 4.6. Hydrate cell filled with sand and water 25
Figure 4.7. Top view of the top cover. 26
Figure 4.8. Thermocouples, artificial well, spiral pipe mounted on the top cover .. 27
Figure 4.9. Experimental set-up outside the constant temperature room 28
Figure 4.10. High-pressure gas bottles a) Air, b) Methane 29
Figure 4.11. Back-pressure regulator 30
Figure 4.12. Separator 30
Figure 4.13. Gas flow meter 31
Figure 4.14. Silica gel tube 31
Figure 4.16. Experimental procedure 33
Figure 5.1. Pressure-temperature diagram during hydrate formation stage of Experiment-1 36
Figure 5.2. Pressure decline rate during hydrate formation of Experiment-1 36

Figure 5.3. Pressure – temperature traverse during hydrate formation and gas production stages in Experiment-1 37
Figure 5.4. Pressure and temperature data of Experiment-2 by time..... 39
Figure 5.5 Pressure – temperature traverse during hydrate formation and gas production stages in Experiment-2 39
Figure 5.6. Pressure decline rate during hydrate formation of Experiment-2..... 40
Figure 5.7. Pressure and temperature data of Experiment-3 during hydrate formation..... 41
Figure 5.8. Pressure and temperature data of Experiment-3 during hydrate formation (Stage-a) 41
Figure 5.9. Pressure and temperature data of Experiment-3 during hydrate formation (Stage-b)..... 42
Figure 5.10. Pressure decline rate during hydrate formation of Experiment-3..... 42
Figure 5.11. Change in moles of free gas and gas consumption rate during hydrate formation in Experiment-3..... 45
Figure 5.12. Pressure – temperature traverse during hydrate formation and gas production stages in Experiment-3 45
Figure 5.13. Experiment production stage (Pressure, Temperature, Gas Flow Rate, Cumulative water production vs time)..... 46
Figure 5.14. Experiment-3 thermocouple values in different depths during production 47
Figure A.1. Time steps of 0-8 55
Figure A.2. Time steps of 9-17 55
Figure A.3. Time steps of 18-26 56
Figure A.4. Time steps of 27-35 56
Figure A.5. Time steps of 36-44 57
Figure A.6. Time steps of 45-53 57
Figure A.7. Time steps of 54-62 58
Figure A.8. Time steps of 63-71 58
Figure A.9. Time steps of 72-80 59

Figure A.10. Time steps of 81-89 59
Figure A.11. Time steps of 90-98 60
Figure A.12. Time steps of 99-107 60
Figure A.13. Time steps of 108-116 61
Figure A.14. Time steps of 117-125 61
Figure A.15. Time steps of 126-134 62
Figure A.16. Time steps of 135-143 62
Figure A.17. Time steps of 144-152 63
Figure A.18. Time steps of 153-161 63
Figure A.19. Time steps of 162-170 64
Figure A.20. Time steps of 171-179 64
Figure A.21. Time steps of 180-188 65
Figure A.22. Time steps of 189-197 65
Figure A.23. Time steps of 198-206 66
Figure A.24. Time steps of 207-215 66
Figure A.25. Time steps of 216-224 67
Figure A.26. Time steps of 225-228 67

LIST OF ABBREVIATIONS

ABBREVIATIONS

(#)L	Liter
BPR	Back Pressure Regulator
D	Diameter
L(#)	Length
n	mole(s)
P	Pressure
PT	Pressure Transmitter
T	Temperature
TC	Thermocouple
V	Volume
Z	Gas compressibility factor

CHAPTER 1

INTRODUCTION

As our civilization has been developing, energy became the main source of its subsequent growth. Fossil fuels are one of the major energy sources with the industrial revolution for several purposes from heating to transportation. After facing serious consequences of increase in greenhouse effect, demand for the fossil fuels, which are harmful to the environment, is decreasing. In order to achieve aims of Paris Agreement, emissions need to fall to 9.7 Gt in 2050 for an emissions pathway compatible with the 2 °C target (Gielen et al.,2019). However, the demand on the natural gas in the category of fossil fuels is likely to be higher since it is less harmful to the environment, and pollutes air less. That is why natural gas tends to sustain its popularity comparing to other fossil fuels. Also, it can help to support countries' policies that are involved to United Nations Framework Convention on Climate Change with the number of 197 member parties. Moreover, it is predicted that natural gas demand will increase until 2040 according to stated policies scenario of IEA, 2020. The increasing trend in natural gas demand may require new but unconventional gas resources to supply the demand. Natural gas hydrate reserves are estimated to contain highest amount of gas among all other unconventional sources.

For the last 30 years more and more researchers try to understand the function of gas hydrates in different fields of their use. This results in a significant increase in the research work about the structural, thermodynamic and kinetic parameters that affect the function of gas hydrates (Sotirios and Parlaktuna, 2021). There are several laboratory studies carried out on the gas production from hydrate reservoirs using different scales, since the amount of gas estimated to be present in the

methane hydrate reservoirs is very high and production schemes from these reservoirs will be different from today's known gas production techniques.

This study will investigate experimentally, two possible gas production mechanisms, namely thermal stimulation and depressurization, from hydrate bearing reservoirs.

CHAPTER 2

LITERATURE REVIEW

2.1 An unconventional natural gas resource: Natural gas hydrates

The natural gas resources can be classified into two parts; conventional and unconventional. The main classification is the permeability of the zone where natural gas is present. It is classified as conventional resources when the resource permeability is medium or high, otherwise it is called unconventional resources which have low permeability.

Conventional natural gas resources, which have high or medium permeability quality, are presented in small volumes and are easy to develop (Figure 2.1). On the other hand, unconventional natural gas resources, which have low permeability, are presented in large volumes but are difficult to develop because of the increase in price and technological challenges (Ahmed and Meehan, 2016). Gas hydrate reservoirs are known as unconventional natural gas resources.

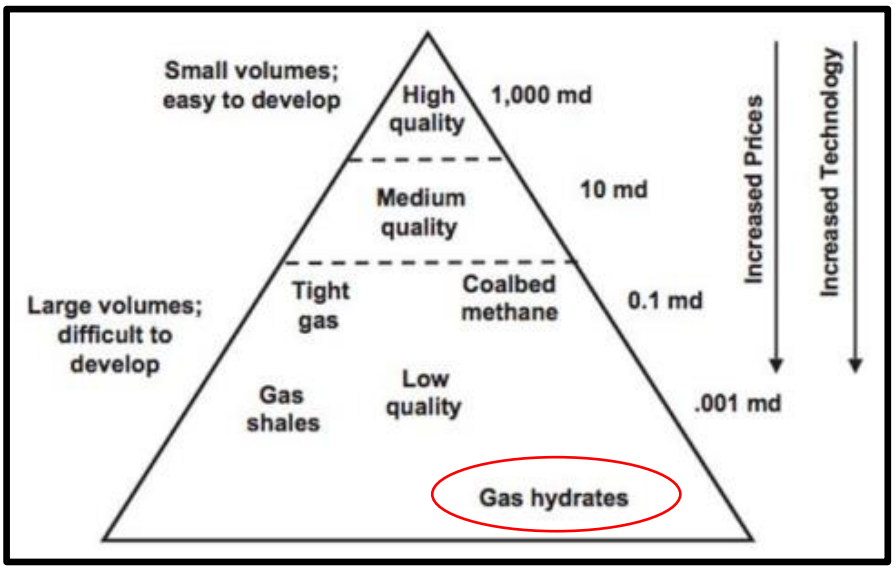

Figure 2.1. Resource Triangle for Natural Gas (Holditch, 2006)

According to the United States Geological Survey, the world's gas hydrates may contain more organic carbon than the world's coal, oil, and other forms of natural gas combined. Estimates of the naturally occurring gas hydrate resource vary from 10,000 trillion cubic feet to more than 100,000 trillion cubic feet of natural gas (EIA, 2012). For example, there is a high producible gas hydrate potential (~ 98.16 standard trillion cubic meter) in the Mediterranean Basin (Merey and Longinos, 2019). Conventional natural gas reservoirs contain free gas in the porous environment under cap rock as well as dissolved gas in crude oil and / or formation water, and natural gas is produced by pressure drop created by wells drilled to the reservoir level. In gas hydrate reservoirs, all or the majority of natural gas is trapped in molecular lattice structures formed by hydrogen bonds by water molecules. In order to produce natural gas from the solid phase, lattice structures need to be dissociated. Dissociation of lattice structures is possible by changing thermodynamic conditions (high pressure and low temperature conditions).

2.2 Natural gas hydrate structures and classes

Gas hydrates are crystalline structures that form in the existence of water and gas molecules which is known as guest molecule at relatively low temperature (generally above the water's freezing point) and high pressure. Depending on the size of the guest molecule, gas hydrates might have different lattice structures. Figure 2.2 shows the gas hydrate structures (Sloan and Koh, 2008).

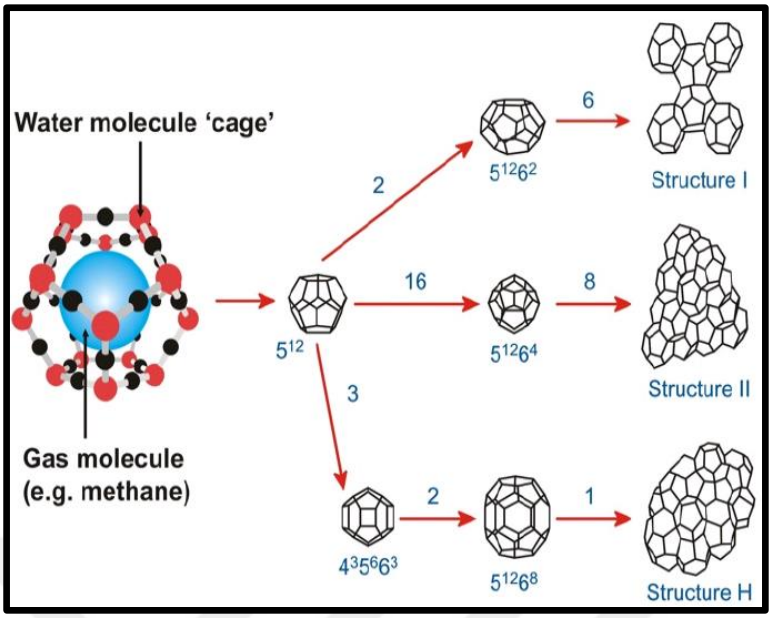

Figure 2.2. Gas hydrate structures (Sloan D and Koh CA, 2008)

Those structures are listed as

- Structure I: It contains 46 water molecules per each unit cell with two dodecahedral and six tetrakaidecahedral voids. It is formed by methane (CH_4), ethane (C_2H_6), carbon dioxide (CO_2) and hydrogen sulfide (H_2S).

- Structure II: It contains 136 water molecules per each unit cell with sixteen dodecahedral and eight hexakaidecahedral voids. It can be formed by propane (C_3H_8) and iso-butane (C_4H_{10}).

- Structure H: It is the less common structure. It contains 34 molecules per unit cell with three pentagonal, two irregular dodecahedral and one icosahedral voids. (Koh et al., 2009).

While the structure I type gas hydrate contains 46 water molecules and 8 gas molecules, the structure II type gas hydrate contains of 136 water molecules and 24 gas molecules, which gives the ratio of the hydration number 5.75 and 5.67, respectively, when all the cages have been totally occupied by the gas.

Natural gas hydrate deposits can be divided into four main classes as shown in Figure 2.3 (Lee et al., 2011). First three classes have overburden and underburden layers, but Class-4 consists only hydrate bearing layers.

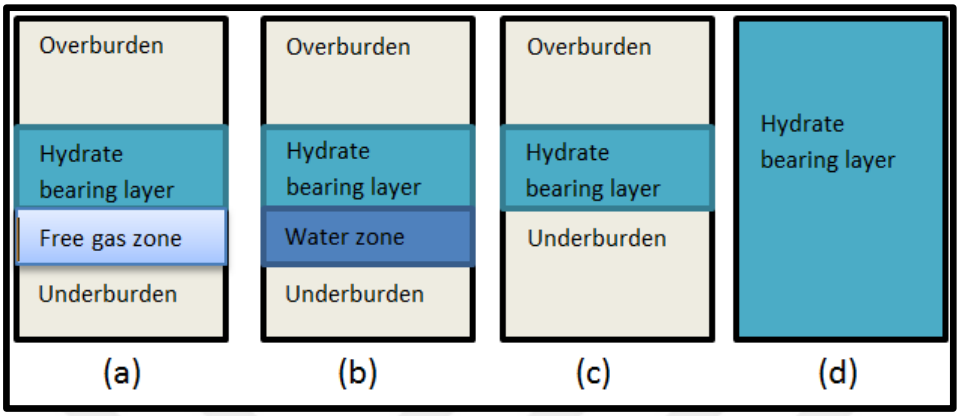

Figure 2.3. Hydrate classes; (a) Class-1, (b) Class-2, (c) Class-3, (d) Class-4 (Lee et al., 2011).

- Class 1: Such structures have two different zones. Those are the hydrate zone at the top of the structure and the two-phase (water and free gas) fluid zone below it. The hydrate zone often has very low active permeability values due to high hydrate saturation. In Class 1 hydrate reservoir, the base depth of the hydrate stability zone coincides with the base of the hydrate zone. Class 1 hydrate reservoirs are considered as the most suitable reservoirs for gas production since the thermodynamic conditions in the reservoir are very close to the hydrate equilibrium conditions. (Moridis et al., 2007). It is possible to initiate the hydrate degradation by changing the pressure and / or temperature in small quantities.

- Class 2: Although there are two different zones like in Class 1, there is an aquifer under the hydrate zone that does not contain free gas and it is only saturated with water.

- Class 3: This class consists of a single hydrate zone but no underlying fluid-saturated layer.

- Class 4: This class consists of only hydrate bearing layer which could be found some of the marine hydrate reservoir. It is the less effective in depressurization since production of water is too much comparing to the gas produced. (Moridis and Sloan, 2007).

Hydrate classes described above have significant effects for the determination of production strategy.

2.3 Formation – dissociation of hydrate

In order to produce methane and water from the hydrate, hydrate formed should be preserved under specific temperature and pressure conditions in the laboratory. Natural gas hydrates are formed by trapping gas molecules of appropriate size in the lattice structure formed by water molecules. High pressure and low temperature conditions are essential for this formation. Earlier studies revealed that hydrate formation takes not only hours or days but weeks maybe months in order to mature. This maturation is known as induction period. Hydrate formation is only possible when both pressure and temperature condition are in the hydrate region which is the region highlighted in yellow in Figure 2.4. The boundary between hydrate and non-hydrate region is known as equilibrium line (red line in Figure 2.4). The hydrate equilibrium line shown is Figure 2.4 was derived using the CSMHYD software (Sloan, 1990).

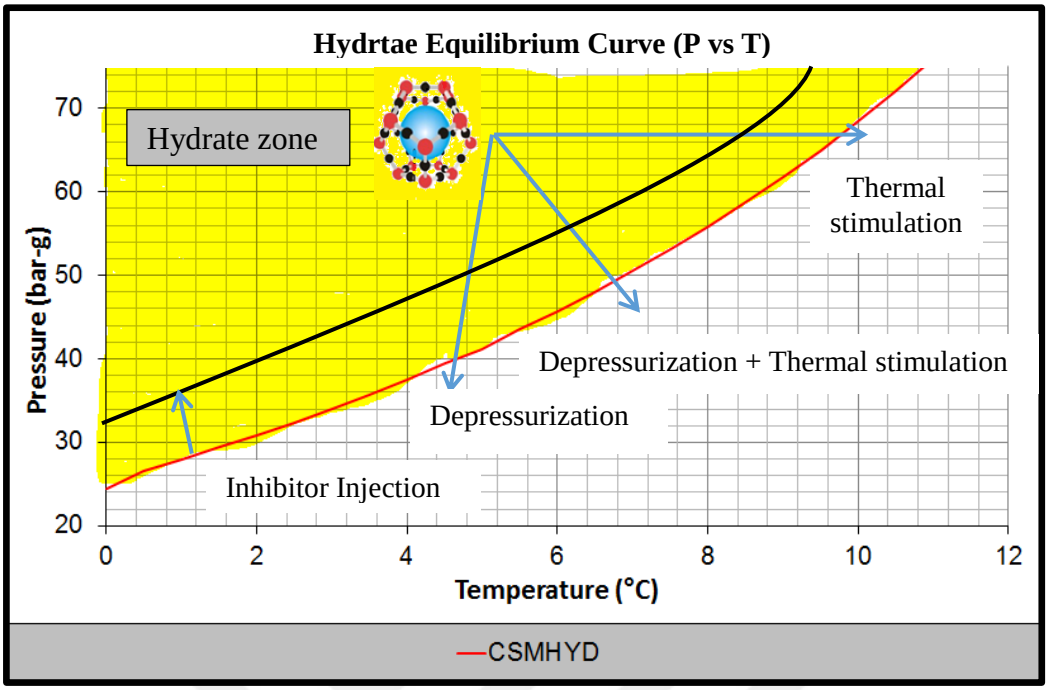

Figure 2.4. Hydrate equilibrium curve of pure methane

Figure 2.4 shows possible production schemes (thermals stimulation, depressurization and inhibitor injection) of gas production from hydrate reservoirs. Thermal stimulation techniques encompass all methods of releasing gas by increasing the temperature of the hydrate reservoir. The temperature increase can be achieved by circulating the hot water/steam pumped into a well in the reservoir or by a heater lowered into the well. Depending on the method applied, the temperature increase may be limited to the well vicinity. Alternatively, larger areas can be heated by water flooding from the injection well to the production well in the reservoir. Whichever method is used, the aim is to increase the temperature of the reservoir to a value above the hydrate equilibrium temperature, and to allow the gas to flow towards the production well.

In the depressurization method, the hydrate is dissociated by reducing the pressure in the bottom of the well without changing the reservoir temperature. In this method, production first starts around the well, and then, with the increase in permeability due to the dissociation of the hydrate, the dissociation spreads to away from the well.

Thermal recovery methods can be considered as more effective method than depressurization method. However, since dissociation of hydrate is an endothermic reaction, the heat supplied to the reservoir must be regular and uninterrupted in order for this effect to be maintained. Otherwise, the reservoir reaches the equilibrium temperature again and the gas flow is interrupted. Although it is an effective production method, it is not always feasible due to the disadvantage of high cost of thermal recovery methods. For example, one liter of water has to receive 4184 Joules for 1°C increase in its temperature, which may cost a lot when the application volume in the reservoir conditions is considered.

Inhibitor injection method shifts the hydrate equilibrium curve (red line) to the left (black line) by lowering the hydrate equilibrium temperature of a given pressure. If the temperature and pressure conditions of a water – gas system becomes outside the new hydrate formation zone after the shift, the thermodynamic conditions allow hydrates to be dissociated.

CO2 or CO2/N2 injections are similar to inhibitor injection in terms of change in equilibrium curve. Since the injected gas or gas mixture will form hydrate, heat is released. Although the geo-mechanical structure of the sediment is preserved in this method and it provides an opportunity for injected gas storage. The successful application of the replacement technique by using a binary CO2–N2 gas mixture on the Alaska North Slope in the United States demonstrated the feasibility of this technique in the field (Boswell et al., 2016).

2.4 Natural gas hydrate laboratory studies in porous environment

As hydrate reservoirs are porous environments like shallow marine sediments, there will be discussions about laboratory studies in porous environments for hydrate formation and gas production in the literature.

Tang et al. (2005) formed methane hydrate in a one-dimensional apparatus that is filled with 300 - 450 micrometer (μm) sized compressed dry sand and saturated

with brine containing 2% by weight salt (NaCl) in a media of 30% porosity and permeability of 0.11 Darcy. Then, the back-pressure regulator at the exit point was adjusted to a 0.1 MPa higher than the cell pressure and the outlet valve was opened and the gas was produced by using steam / hot water mixture in the inlet line. During production period, temperature changes, production rates of gas and water and the efficiency of thermal stimulation were monitored. Gas production, which showed a sudden increase at the early stage of production, immediately decreased. However, water production remained constant throughout the experiment. As a result of the study, the factors that affect the ratio of the energy that can be obtained from the gas produced to the energy consumed to produce the gas are determined as the temperature of the water, the water flow rate that goes into the cell and the hydrate saturation.

Bai et al. (2009) used 38 × 38 × 18 cm rectangular prism hydrate cell with a working pressure of 15 MPa to study pressure reduction method. The porosity and the permeability of the 300 - 450 μm compacted dry sand was measured as 30% porosity and 1.97 Darcy, respectively. Prepared under high pressure with pure water and methane gas, the temperature of the system was lowered by lowering the air bath temperature below the equilibrium temperature to form the hydrate. After 2 - 3 days spent in the hydrate formation process, outlet pressure of the cell was reduced below the hydrate equilibrium pressure and gas production and hydrate dissociation were realized.

Linga et al. (2009) worked 150 - 630 μm (average 390 μm) filled with silica, pure water and methane in a porous environment under the pressure of 49 bars and hydrate was formed. Then, during gas production stage, changes in the dissociation rate of the hydrate were observed by raising the temperature above the equilibrium temperature using a constant temperature air bath. Gas production started quickly but then slowed down. There is an approach that the hydrate formation cell diameter is changed with the copper cylinders. In 3 experiments with this approach, the hydrate volume was changed while keeping the porous media height constant at 7 cm. The study concluded that the gas production process occurs in two different

stages. In the first stage, gas production rate changes with volume of hydrate formed. Gas production rate is not related to the hydrate volume formed in the second stage of the production.

Du and Feng (2010) examined the effects of a thermodynamic inhibitor, Ethylene Glycol (EG), on hydrate dissociation with same experimental set-up used by Bai et al. (2009). EG was injected at different concentrations and flow rates into the cell containing hydrate. Gas production increased while increasing these two parameters. However, it was concluded that the hydrate structure could not be completely dissociated by only thermodynamic inhibitory injection. The main reason for this was that the injected inhibitor reached the production well without contacting the whole hydrate.

Yang et al. (2010) studied production of gas from the porous media containing hydrate by hot water injection in a cylindrical cell with 30 cm in diameter and 10 cm in height under working pressure of 16 MPa. The cell was placed in a bath with ethylene glycol solution to maintain constant temperature conditions. A 3 mm diameter well, located in the center of the cell, was used to inject hot water into cell after the formation of hydrate. At the end of different conditions, it was observed that energy efficiency ratio (cooling capacity to power input) increased with hydrate saturation and hydrate temperature, and decreased with increasing temperature of the injected hot water and well pressure.

Schicks et al. (2011), used a large volume (425 liters) of hydrate formation – dissociation cell - LARS (Large Scale Reservoir Simulator) in their study. It is a cylindrical cell with 60 cm in diameter and 150 cm in height and the pressure in the cell can be increased up to 25 MPa. The cell is equipped with thermocouples and methane detectors in order to see the change of thermal facade and methane concentration in the cell during hydrate formation and dissociation processes. Figure 2.5 shows schematic of experimental set-up.

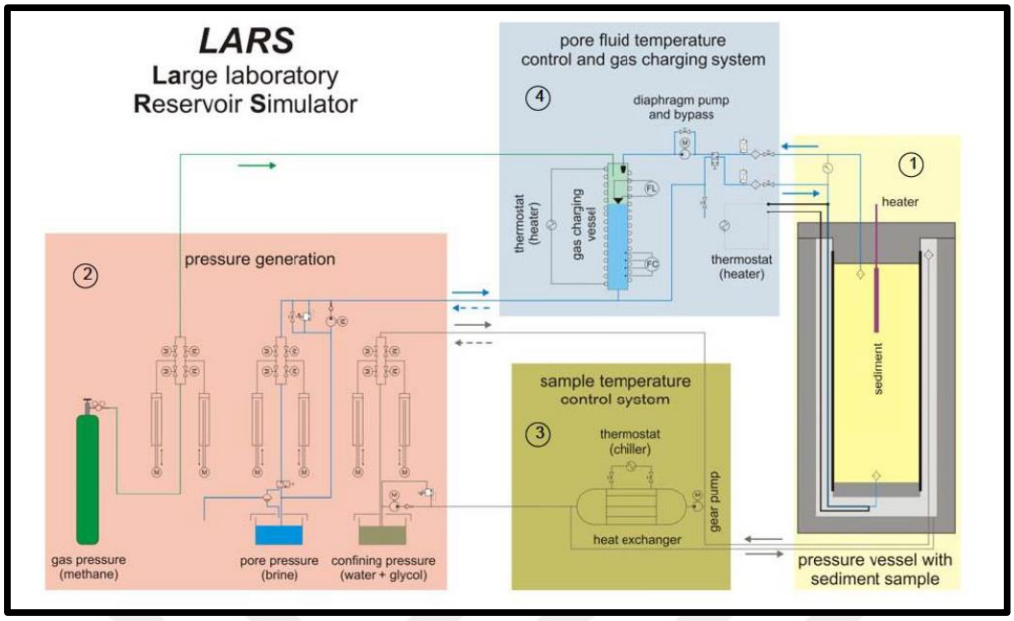

Figure 2.5. Schematic diagram of LARS (Schicks et al., 2011)

The test apparatus enables hydrate formation in the porous medium by four different methods:

1. Methane injection into the frozen system partially saturated with salt water,
2. Methane injection into water saturated system,
3. Water injection into methane saturated system,
4. Water saturated system containing dissolved methane.

Li et al. (2012) introduces the hydrate cell (117.8 l) on a pilot scale. An experiment with working pressure of 30 MPa can be carried out in a constant temperature chamber. The pilot cell has a diameter of 50 cm and a height of 60 cm. In order to produce gas, a well with a diameter of 0.4 cm was placed at the center of the cell and 4 slots were opened for production. During the first experiment, gas production process was started by depressurizing the cell with the first saturation values of 27% hydrate and 37% water. This experiment showed that dissociation facade is a moving boundary, which separates the hydrate-containing zone and the water and gas-released zone after dissociation. While the temperature decreases in the zones

where the hydrate dissociates, it is observed that temperature remains close to the constant in the regions where there is no dissociation.

Xiong et al. (2012) studied hydrate formation – dissociation processes by pressure reduction method in a cylindrical cell with 3.8 cm inner diameter and 25 cm height. Hydrate was formed under 25 MPa working pressure, using pure water and methane (Figure 2.6).

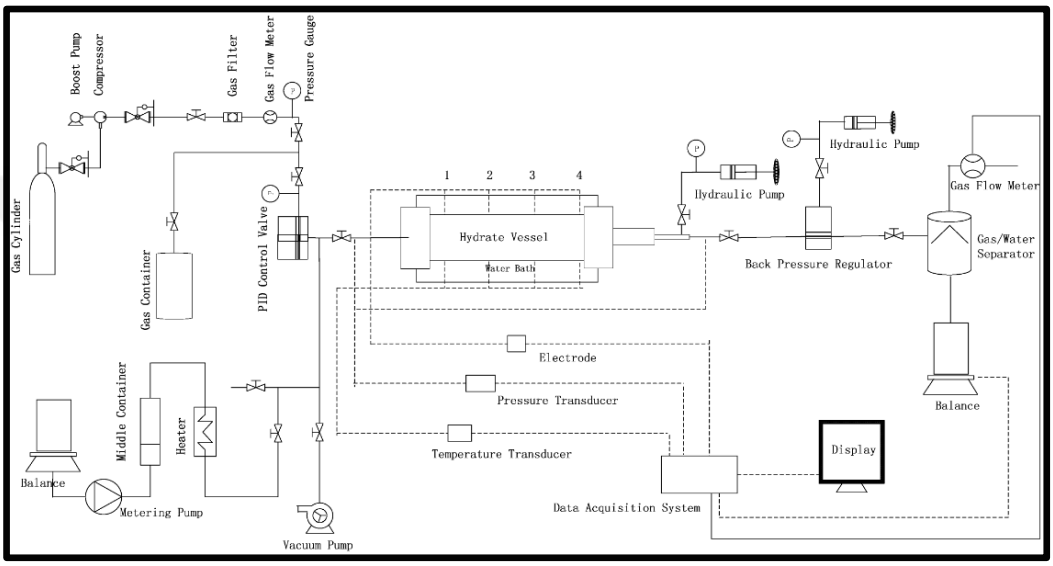

Figure 2.6. Schematic diagram of experimental set-up (Xiong et al., 2012)

They performed temperature and self-resistance measurements. When the results of the experiments are examined, the data of temperature, self-resistance and gas production rates show that hydrate dissociation process takes place in three different stages; production of free gas, fast dissociation, and slow dissociation. Experimental results show that the rate of dissociated hydrate in the fast dissociation phase decreases with increasing hydrate saturation. By decreasing the dissociation pressure, the dissociation rate and dissociation temperature increase. On the other hand, the decrease in dissociation pressure works against secondary hydrate formation.

Yang et al. (2012) produced gas by pressure reduction method with the same mechanism they used in 2010. Experimental results showed that hydrate

dissociation occurs in the whole hydrate zone, and controlled by mass and heat transfer. Thermal buffer formation was observed during the hydrate dissociation process in the 271.5 - 272.2 K temperature range. The ice formed after the dissociation of the hydrate slows the hydrate dissociation rate under the icing temperature and affects the gas production rate. At the end of all these observations, it is recommended to use the pressure reduction method at the beginning of the production process, and then to apply one of the thermal stimulation methods.

Fitzgerald and Castaldi (2013) used a 59.3 liter cylindrical high pressure cell in their studies. In the porous medium formed with quartz particles with an average diameter of 500 μm, hydrate was formed with saturation values of 10% and 30% by the help of pure water and 99.97% purity methane gas. Heat recovery experiments were carried out using heater, which can be used in the range of 0 - 250 W, placed in the middle of the cell. In the hydrate formation process, the presence of a secondary hydrate formation front observed when the test period was long. On the other hand, during dissociation experiments, it has been shown that increasing the hydrate saturation increases the energy efficiency as a result of the experiments carried out at low heating rates such as 20 W and 100 W.

Konno et al. (2014) used a 1710 liter HIGUMA cell in their studies. As a result of their experiments, it was found that even if no ice formation was observed during the gas production with pressure drop, the temperature decrease had a negative effect on the gas production, and it decreases production rate. Also, it was noted that although ice formation during gas production is clogging the pores and reducing the permeability, the heat generated by the exothermic reaction of the ice formation positively affects gas production.

Li et al. (2014) showed that the slow decrease of pressure during the gas production caused high water production, in a high pressure cell with the volume 117.8 liters.

Örs and Sınayuç (2014) examined the replacement process of methane in the hydrate phase and carbon dioxide in the gas phase (Figure 2.7).

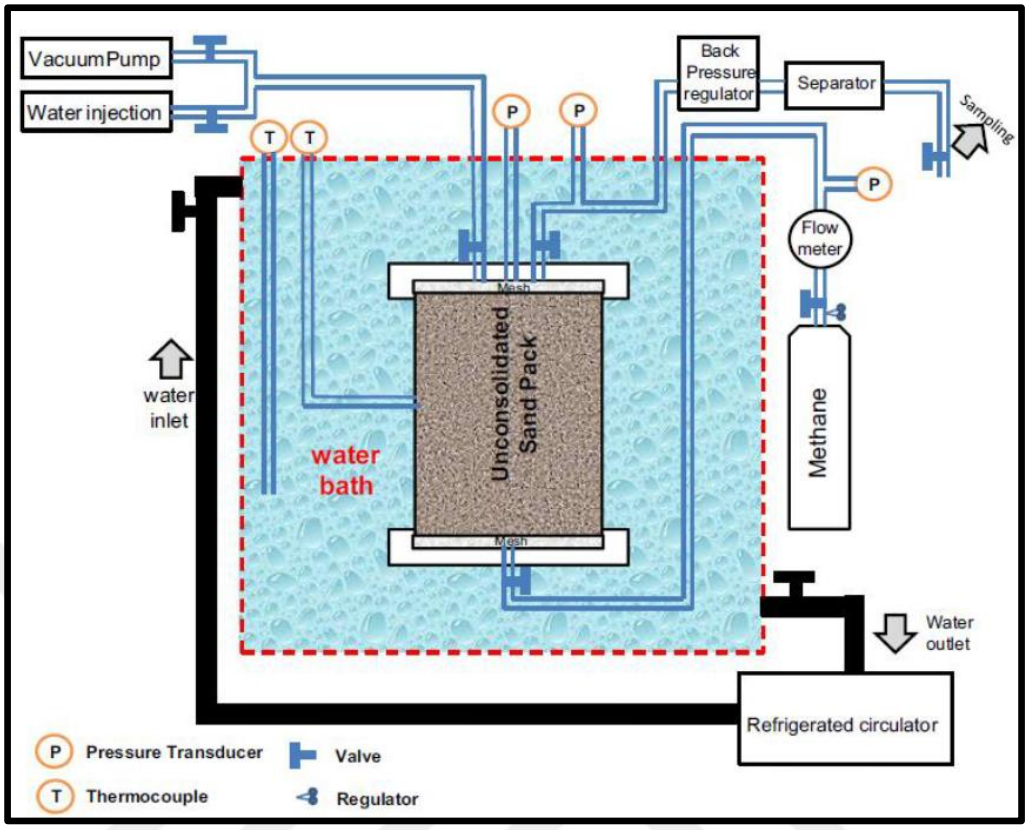

Figure 2.7. Schematic diagram of experimental set-up (Örs and Sınayuç, 2012)

Using sand particles (grain size in the range of 0.25 - 0.50 mm), porous media was created in a cell with volume of 670 cm^3. The porous medium was prepared with high pressure methane at 30% saturation and the hydrate formation process was carried out by replacing the spent methane with methane for several times and all the water in the cell was spent for hydrate to be formed. Subsequently, a known amount of carbon dioxide gas was introduced into the cell to produce methane - carbon dioxide mixture free gas medium. The compositions of the samples, which are taken from the free gas phase immediately after the carbon dioxide gas was injected and during the displacement process, were measured by gas chromatography. The results of the experiments showed that the hydrate cell was filled with 86.3% carbon dioxide.

Cheng et al. (2014) studied the effect of heat transfer from the top and bottom of the hydrate zone in gas production experiments with a pressure reduction using a 5

liter high pressure cell. It is reported that with the start of production, the heat inside the cell is used to dissociate the hydrate, resulting in the formation of ice in the cell and / or in the production line. It has also been shown that temperature increases are observed locally due to the heat released by the ice formed, and there are increases in gas production in proportion to this, but the general tendency is to decrease the gas production rate.

Feng et al. (2015) changed the cylindrical cell that was previously used by Li et al. (2010 and 2012). With a cubic cell of an edge length of 18 cm, two horizontal wells for hot water injection and for gas-water production were placed in the cell with an active volume of 5,835 lt. Energy efficiency ratios showed that hot water injection and pressure reduction with the application of horizontal wells for gas production are promising techniques. The increase in hot water injection temperature increased the gas production rate for a short time but caused a significant decrease in the energy efficiency. On the other hand, decreasing the permeability value of the reservoir caused the energy efficiency to decrease, and the time required for dissociation increased.

Nair et al. (2016) used a 759 ml cell in their experimental studies. By placing four thermocouples at different depths, it is aimed to record the change of thermal facade in hydrate formation and dissociation processes. In the experiments, silica particles of four different sizes (0.16 mm, 0.46 mm, 0.65 mm and 0.92 mm) were used to provide porous media in order to investigate the effect of grain size. In the experiments, methane hydrate was formed using 70% saturation pure water or brine. Hydrate formation in all experiments was kept at 277.15 K and 8 MPa conditions. Gas consumption was found to be higher in the small particle size porous environment than in the large particle environment. It was determined that the total amount of gas consumed in the experiments carried out with salt water was less than the experiments with pure water. Hydrate dissociation was carried out by increasing the temperature from 277.15 K to 303.15 K over a period of two hours. The fastest dissociation rate was achieved at pressure and temperature values close to the hydrate equilibrium conditions.

Song et al. (2016) studied the production of gas by pressure reduction, thermal recovery and combined recovery methods from a hydrate reservoir using a polyamide cell with a total volume of 34.35 ml, 15 mm in diameter, 200 ml in length, and a working pressure of 12 MPa. At the end of seventeen different experiments, it was observed that the combined recovery method using pressure reduction and thermal recovery techniques was higher than the two methods alone.

Abbasov et al. (2016) studied process of carbon dioxide in the hydrate structure of mixture of methane-propane-carbon dioxide by using the setup used by Örs and Sınayuç (2014). Different experiments have shown that the interaction of the hydrate structure with the carbon dioxide-rich free gas can produce methane and propane from the hydrate phase.

CHAPTER 3

STATEMENT OF THE PROBLEM

Natural gas hydrate occurrences are considered as one of the future methane sources of mankind, although there is no commercial realization yet. It is considered that the production process is more difficult than other sources in terms of technology and cost, comparing to other unconventional resources such as tight gas, coalbed methane, gas shales. Despite difficulty of recovery from gas hydrate reservoirs, the amount of gas of this type resource is much greater than the amount of conventional natural gas. And, intensive studies are being carried out on the development of natural gas production technologies from hydrate structures.

Gas production from hydrate reservoirs requires the dissociation of in-situ hydrate by means of external energy supplied which can be achieved by thermal stimulation, depressurization and inhibitor injection. Literature indicates that none of these techniques is the sole solution of the hydrate dissociation and they must be used simultaneously. This thesis aims to investigate the effectiveness of two possible production mechanisms of hydrates, namely depressurization and thermal stimulation, with an experimental study. Methane hydrates will be formed in a porous media formed by crushed – unconsolidated sand particles. Then two different production schemes (depressurization + thermal stimulation and depressurization alone) will be applied to produce gas from hydrate reservoirs.

CHAPTER 4

EXPERIMENTAL SET-UP AND PROCEDURE

As discussed in previous chapters, hydrate formation and dissociation is studied experimentally in this thesis. In order to achieve the goals of this study, hydrates must be formed at first. Then, different gas production schemes should be applied to dissociate the hydrate. This chapter discusses the experimental set-up and procedure.

4.1 Experimental set-up

The experimental set-up shown Figure 4.1 was used during hydrate formation and gas production periods of the study. The laboratory where the whole set-up is situated is divided into two different rooms next to each other: 1) constant temperature cold room and 2) ambient temperature room. The temperature of the constant temperature cold room can be set and kept at a temperature between – 5 °C and +25 °C. High pressure hydrate cell, water circulation bath and the data recorder are the main components situated in the cold room. Methane and air high-pressure gas bottles, a second data logger, separator, gas flow meter and back-pressure regulator are the components located in the ambient temperature room. Those components, except high-pressure gas bottles are mainly utilized during gas production.

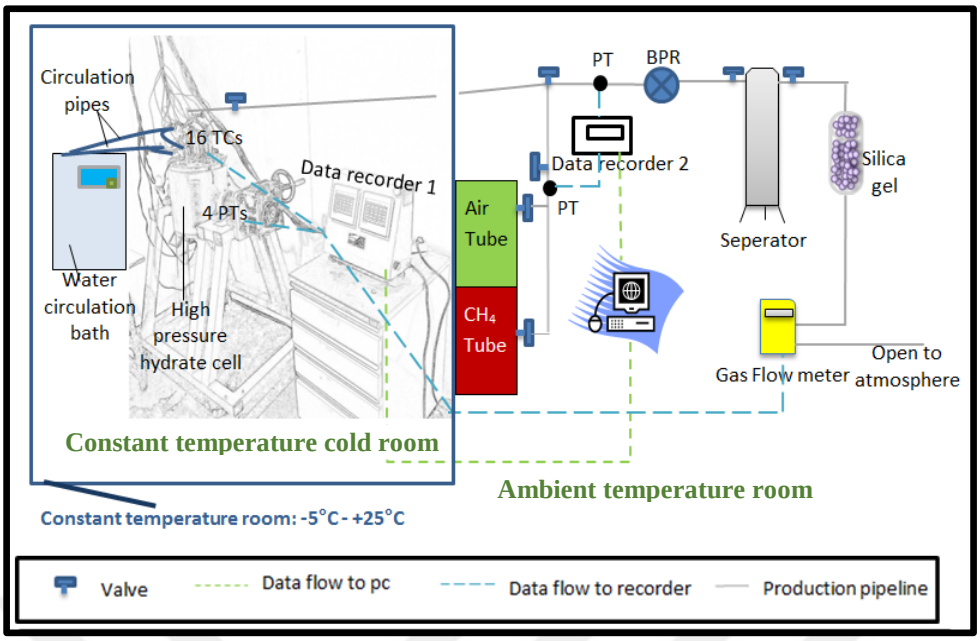

Figure 4.1. Experimental set-up

4.1.1 Constant temperature room

High pressure and low temperature conditions are the two main conditions to from hydrate. In that respect, a high-pressure cell is always present as the main component of a hydrate formation set-up. Regarding the low temperature condition, two main paths are followed in the literature: there are experimental set-ups in which only the high-pressure cell is situated in a constant temperature air bath (Bai et al., 2009) or ethylene glycol solution bath (Yang et al., 2010), or constant temperature rooms where the whole set-up is kept at low and constant temperature (Linga et al., 2009). The second option is the choice of this study. A 9 m^2 (3 by 3 m) constant temperature room with 2.5 m height was utilized to situate the hydrate formation set-up of the current study (Figure 4.2). The temperature of the room can be controlled within the range of -5 °C - + 25 °C with an accuracy of ± 1 °C.

Figure 4.2. Constant temperature room

Figure 4.3 shows the basic components of the experimental set-up situated in the constant temperature room such as high-pressure hydrate cell, data recorder-1, rotation unit and frame.

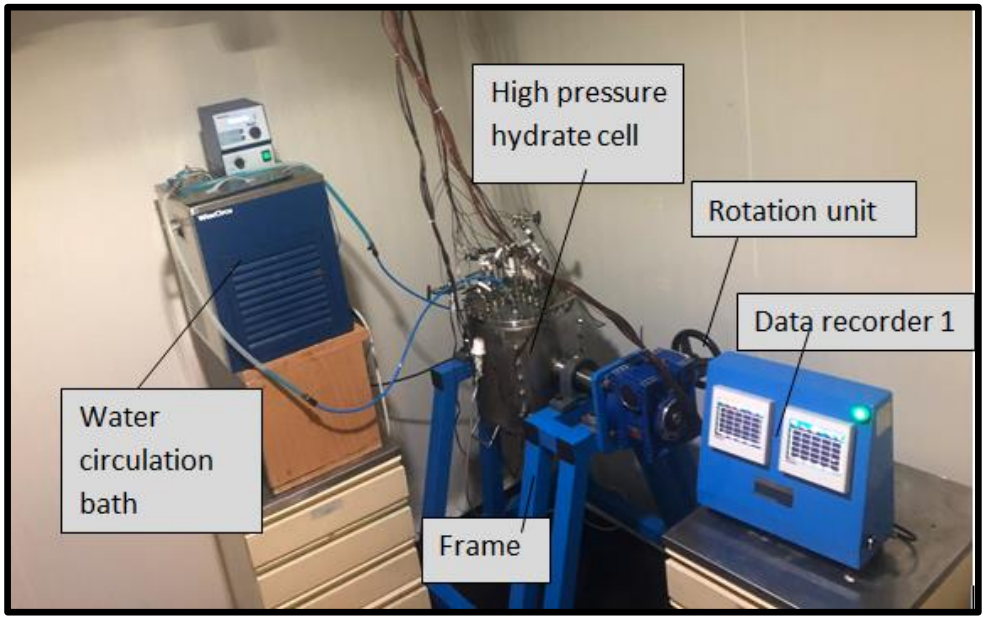

Figure 4.3. Components situated in the constant temperature room

A cylindrical high-pressure cell whose dimensions given in Table 4.1 is utilized for hydrate formation (Figure 4.4).

Table 4.1 Measurements of cylindrical high pressure hydrate cell

Name	Volume (L)	Diameter (cm)	Height (cm)	Design pressure (bar)
Cylindrical high pressure hydrate cell	21.62	30	30.63	200

Figure 4.4. Cylindrical high pressure cell used for hydrate formation experiments

In order to simulate the hydrate formation in nature, high-pressure cell is filled with crushed limestone to create a porous medium (Figure 4.5 and Figure 4.6).

Figure 4.5. The sand filling the hydrate cell

Figure 4.6. Hydrate cell filled with sand and water

The high-pressure cell is equipped with pressure transducers and thermocouples to measure the cell pressure and temperature during the hydrate formation - dissociation processes. Four pressure transducers with a measuring range of 0 – 160 bar are mounted to the cell, one on the top cover, two on both sides of the cell and one on the bottom cover. On the other hand, 16 thermocouples, all mounted on the top cover, are used for temperature measurements. In order to obtain temperature a distribution at different depths and in different spatial distribution, those thermocouples are located in a certain order on the top cover. As shown in Figure 4.7. 16 thermocouples within groups of four are immersed into porous medium to the depths of 6 cm, 12 cm, 18 cm and 24 cm from the top cover.

A cm long 1/4-inch steel pipe is attached to the center of the top cover to provide a conduit (artificial well) for the gas production. There are 3 more ports on the top cover, one to attach upper pressure transducer and the remaining two are used to connect the spiral pipe to circulate warm water for thermal stimulation scheme of gas production (Figure 4.7).

Figure 4.8 shows the top cover with all 16 thermocouples, artificial well and spiral pipe for warm water circulation.

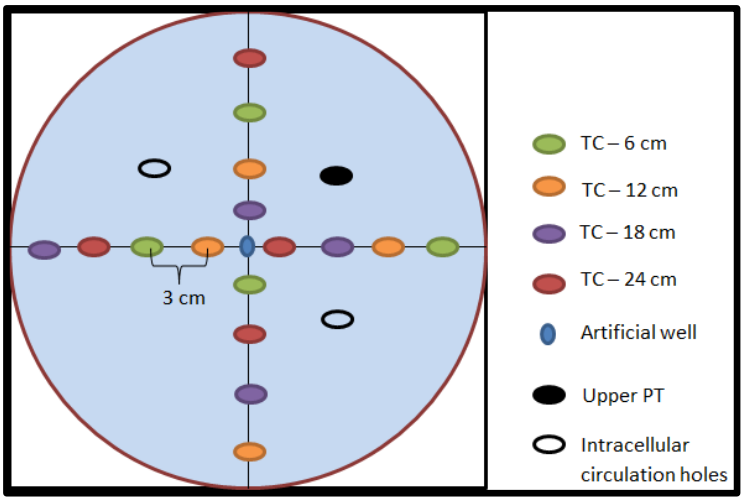

Figure 4.7. Top view of the top cover.

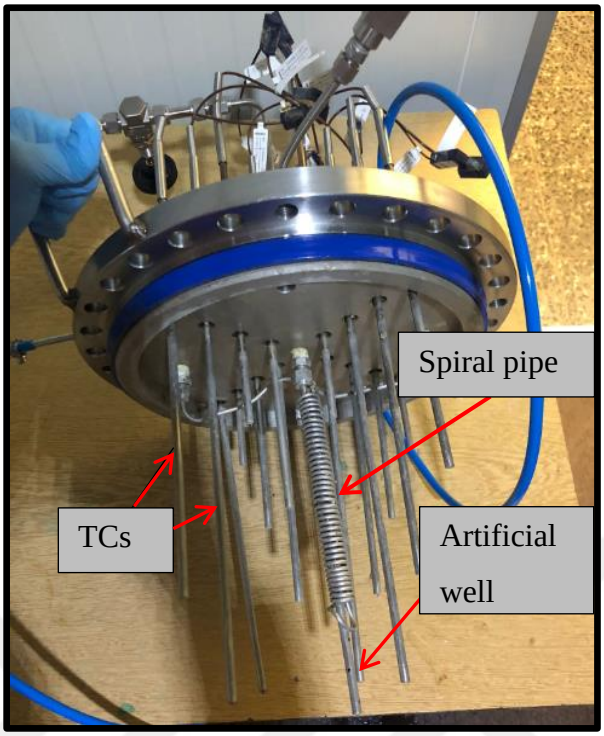

Figure 4.8. Thermocouples, artificial well, spiral pipe mounted on the top cover

During the hydrate formation and dissociation processes, the cell pressure and temperature values, gas flow rate are recorded every 5 seconds by means of Data Recorder – 1 (Figure 4.3).

The frame and the rotation unit are used to carry the heavy high-pressure hydrate cell and to make it upside down to clean the cell after finalizing the cell. This rotation unit was also used to agitate the fluids inside the cell during hydrate formation (Figure 4.3).

As mentioned earlier, it is aimed to test the thermal stimulation scheme for gas production from hydrate reservoirs which require heat input into the cell. This was achieved by means of warm water circulation through spiral pipe by the help of water circulation bath.

4.1.2 Ambient temperature room

As mentioned earlier, gas production activity from high pressure hydrate cell is controlled in ambient temperature room. In addition, two high-pressure gas bottles (air and methane) are also placed in the ambient temperature room. Figure 4.9 shows all the components of experimental set-up located in ambient temperature room which are placed next to the wall of constant temperature room and holes drilled into this wall were used to make all connections between two room (cables, pipes). Descriptions and use of all components are given in the following paragraphs

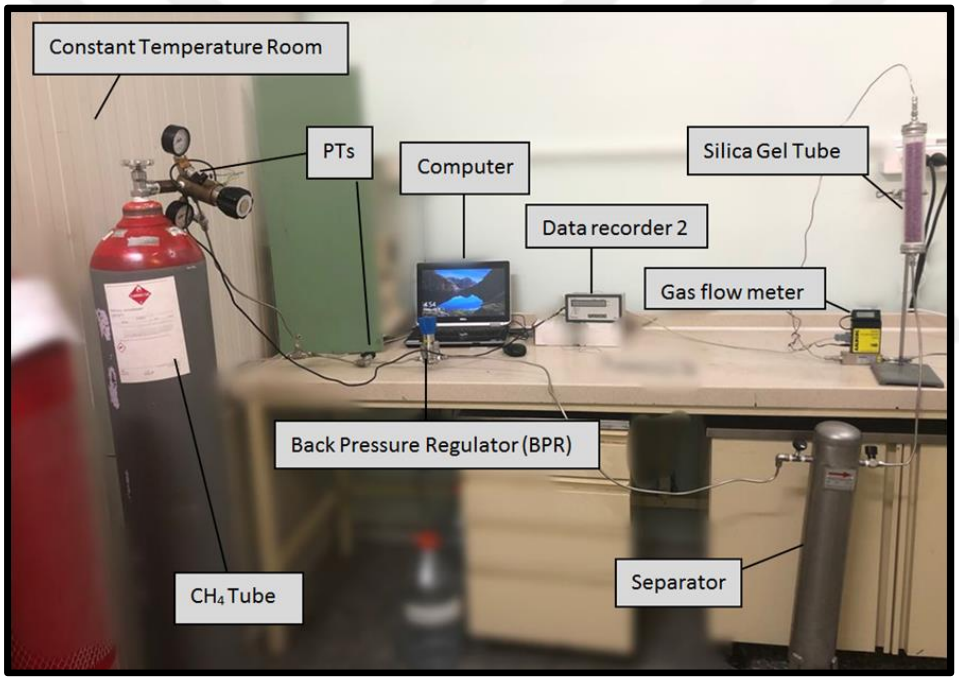

Figure 4.9. Experimental set-up outside the constant temperature room

- High-pressure air bottle: 50-liter high-pressure air bottle is mainly used for leakage control after preparing the system for a new experiment Figure 4.10a).
- High-pressure methane bottle: All hydrate formation – gas production during this study was realized by using pure methane. A 50-liter high-

pressure methane bottle with a purity of 99.99% was used to supply the methane for experiments (Figure 4.10b).

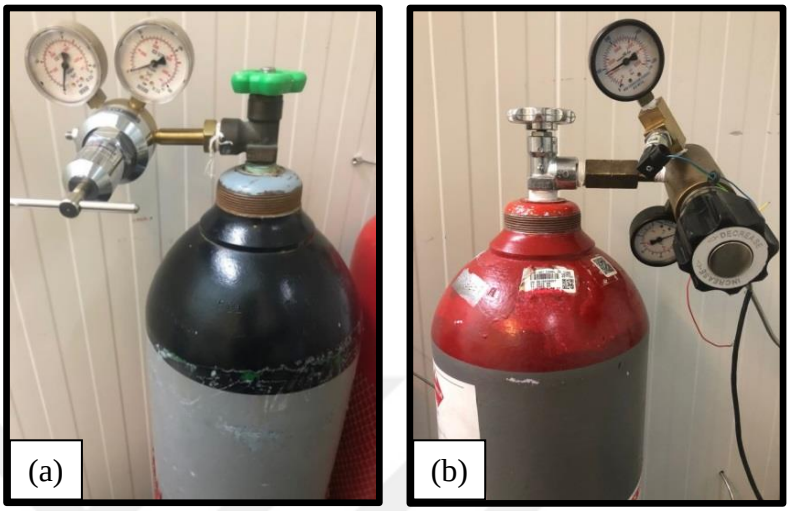

Figure 4.10. High-pressure gas bottles a) Air, b) Methane

- Data recorder-2: This data recorder is utilized the pressure of high-pressure gas bottle and back-pressure regulator set pressure at every 5 seconds.
- Back-pressure regulator: It is the controlling device of gas production process from the high-pressure hydrate cell. Pressure at the inlet of back-pressure regulator is set to al lower pressure than hydrate cell pressure to create pressure drawdown to allow the hydrate dissociation as well as gas flow (Figure 4.11).
- Separator: The separator shown in Figure 4.12 is used to separate gas and water since they leave the hydrate cell together as a response to created pressure drawdown. The separated gas is directed to gas flow meter from the top of separator while the water is collected in the separator. There is a valve at the bottom of separator to drain the produced water at certain intervals before filling the separator.

Figure 4.11. Back-pressure regulator

Figure 4.12. Separator

- Gas flow meter: This device is used to measure the flow of methane gas being produced with a measuring range of 0.0– 35.0 L/min (Figure 4.13).

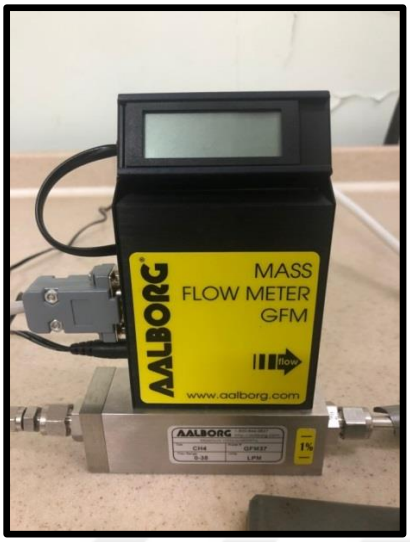

Figure 4.13. Gas flow meter

- Silica Gel Tube: The moisture of produced gas is captured by silica gels filled in a transparent tube to prevent the entrance of water vapor into the gas flow meter (Figure 4.14).

Figure 4.14. Silica gel tube

4.2 Experimental procedure

Two distinct experimental procedures were applied during this study. The first procedure is to form the hydrate from gas – water mixtures in the high-pressure hydrate cell and the second one is to dissociate already formed hydrate into gas and water and produce them by applying thermal stimulation and pressure reduction schemes. But, before applying any of these two procedures, the high-pressure cell must be prepared for the test. The following steps are applied to prepare the cell:

1. Bottom cover of the cell is closed by firmly tightening the bolts.
2. The cell is filled with crushed limestone up to a level 1 cm below the cover to ease the connection of top cover.
3. In the meantime, thermocouples, artificial well and spiral pipe are attached to top cover before closing and tightening the cover.
4. After completing the installation of all connections, gas leakage test is applied by injecting high-pressure air into the cell. The cell is kept under high-pressure for a period of time under constant temperature until a long period of constant pressure conditions is obtained. If a decline in pressure is observed, all the connections are checked by leakage control sprays and necessary interventions are made to stop the leakage.
5. In case of no leakage, high-pressure is released and the cell is filled with water through the valve at the bottom cover. This is done by having a water reservoir which is situated at a level higher than the high-pressure cell and the valve at the top cover is open. Relatively low flow rate of water with the help of gravity fills the pores of the crushed limestone packing. After observing the flow of water from the top valve, the flow is left to flow for 15 minutes. By keeping the balance of injected water, it was possible to determine the porosity of the limestone filled high-pressure cell.
6. Then, the bottom valve is closed and the water reservoir is disconnected.
7. Bottom valve is opened once more to discharge 200 ml water in order to create a space for gas injection through top valve.

8. After discharging 200 ml from the high-pressure cell, the system is ready for gas injection. Then the gas injection line is connected to the top valve and methane is injected into the cell.

Figure 4.16 shows the flow paths of fluids during preparation stage (red arrows) and gas production (green arrows) stages. Experimental procedures during hydrate formation and gas production stages are explained in the following paragraphs.

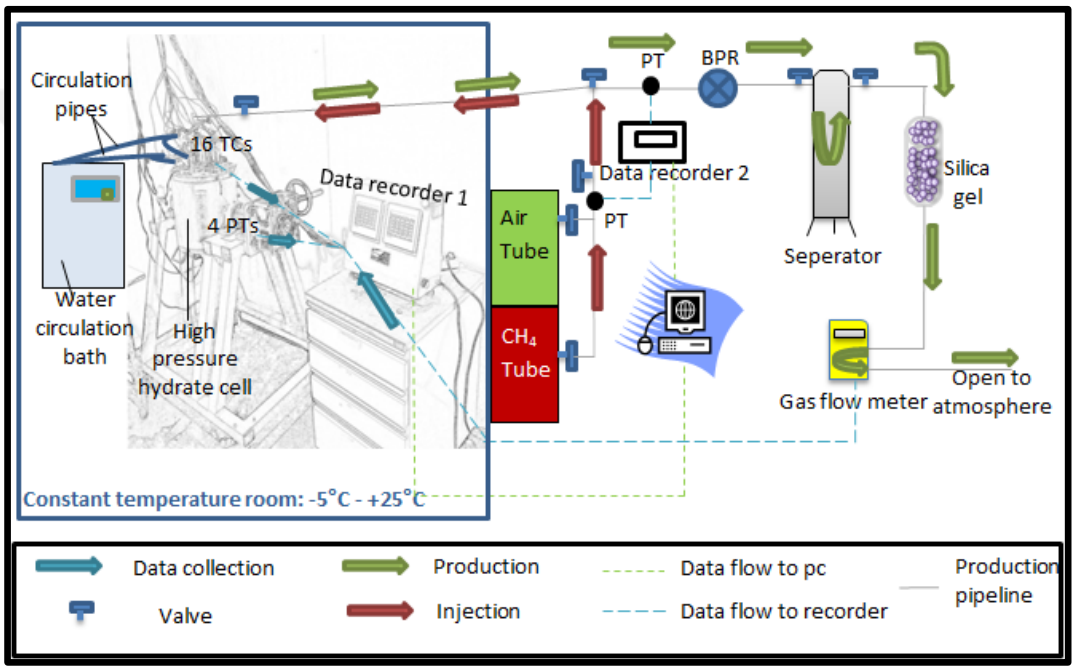

Figure 4.15. Experimental procedure

4.2.1 General procedure for hydrate formation

The following procedure is applied for forming Class 1 gas hydrate in the high-pressure hydrate cell:

1. As explained above, high-pressure hydrate cell is saturated with water and high-pressure methane gas for hydrate formation at the end of preparation activities.

2. Cold room temperature cooler is set to +5 °C then the system is left for cooling to enter into hydrate region of pure methane. Under continuous cooling condition the room temperature is aimed to be kept constant.
3. Temperature and pressure of high-pressure hydrate cell is recorded at every 5 conditions to interpret the hydrate formation process as function of time.

4.2.2 General procedure for gas production

Gas production from hydrate reservoirs necessitate the dissociation of hydrates that were formed in high-pressure hydrate cell. This is achieved by pressure reduction (depressurization) and/or warm water circulation around the artificial well (thermal stimulation). The following procedure is applied for this purpose:

1. The decision to switch from hydrate formation stage to gas production stage is based on pressure vs. time data. This data is first converted into free gas mole vs. time data and interpreted to find the gas consumption rate as function of time. When gas consumption rate becomes low but constant, the hydrate formation stage is stopped and gas production stage is initiated.
2. The top valve on the top cover is opened and the system is expanded up to back-pressure regulator (BPR).
3. High-pressure cell pressure is reduced in a controlled manner by adjusting BPR. Initially the free gas in the cell as well water is produced as a response to the reduced pressure.
4. When the cell pressure becomes lower than hydrate equilibrium pressure hydrate dissociation starts. This process continues by adjusting the set pressure of BPR to lower pressures at each step.
5. During this process, set pressure of BPR and gas flow rate are recorded at every 5 seconds.

CHAPTER 5

RESULTS & DISCUSSIONS

This chapter discusses three hydrate formation – gas production experiments that were carried out by the experimental procedures given in Chapter 4. It is aimed to simulate Class 1 hydrate experimentally by forming natural gas hydrate using pure methane (99.99 %) and tap water. Although both hydrate formation and gas production stages were studied in all three experiments, it was possible to get meaningful gas production data in Experiment-3. Therefore, Experiment-1 and Experiment-2 will be discussed only in terms of hydrate production stage but the whole data of Experiment-3 will be analyzed.

5.1 EXPERIMENT 1

After preparing the high-pressure hydrate cell for gas injection, 3 moles of methane is injected into cell at two steps. In the first step, the cell pressure was increased to a value of 44 bar-g when the cell temperature was about 7.7 °C. This pressure-temperature condition is still outside the hydrate region (Figure 5.1). Then in the second step, by injecting more gas the pressure reached to a value of 69.4 bar-g at 7.1 °C (Figure 5.1). Immediately after, dissolution of gas and decrease in temperature resulted in decline in pressure. At about 3.8 °C the decline in pressure changed its characteristics which is interpreted as the initiation of hydrate formation. The decline is pressure is observed for a period of 56 days, and during this period 6 bar pressure decline was experienced. This decline in pressure in attributed a continuous hydrate formation. In order to decide to cease the hydrate formation stage, the decline rate of pressure is observed (Figure 5.2). As observed, initially there was a rapid decline in pressure but by time the rate slows down and

started to show almost a flat behavior with a very low decline rate. Then, it was decided to stop the hydrate formation stage after day 50.

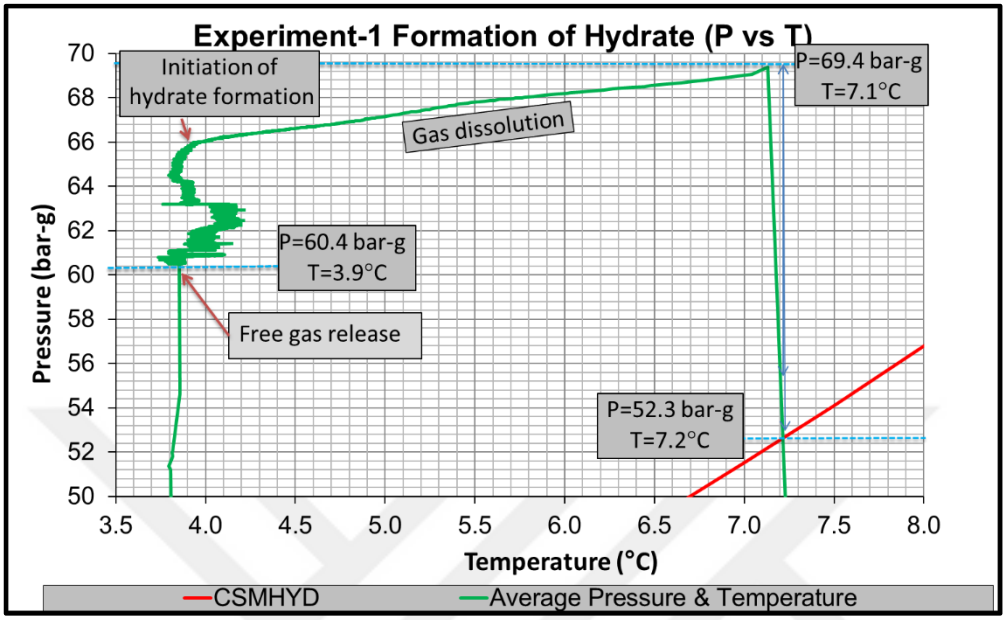

Figure 5.1. Pressure-temperature diagram during hydrate formation stage of Experiment-1

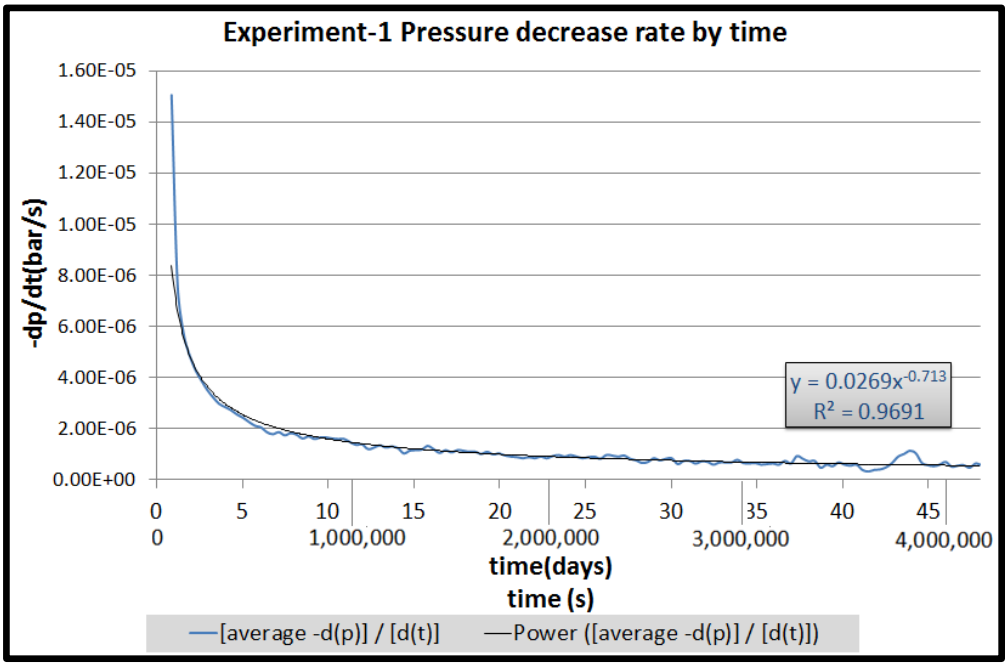

Figure 5.2. Pressure decline rate during hydrate formation of Experiment-1

Figure 5.3 shows the whole pressure-temperature traverse during hydrate formation and gas production stages of Experiment-1. Blue circle indicates the hydrate formation stage. As seen, there exist temperature increase while pressure is continuing to decline. This could be the result of hydrate formation since this hydrate formation is an exothermic process.

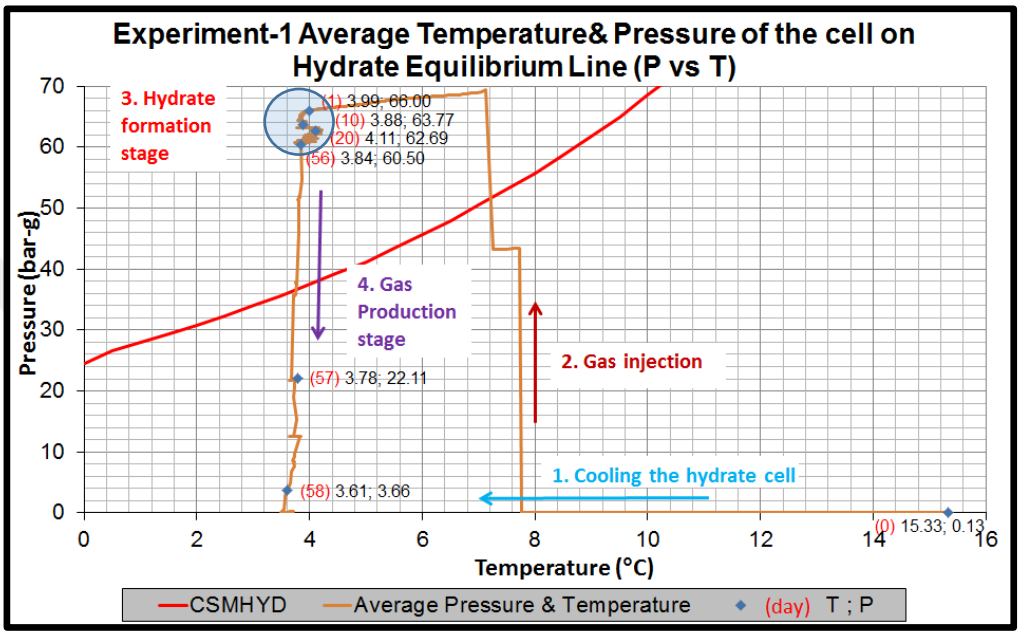

Figure 5.3. Pressure – temperature traverse during hydrate formation and gas production stages in Experiment-1

As shown in Figure 5.3, during gas production stage a sharp decline in pressure is observed with a slight decrease in cell temperature. This is expected since hydrate dissociation is an endothermic process and a decrease is temperature should be observed. Unfortunately, due to problems encountered on the use of separator ruined the gas flow rate measurements. Unexpected overflow of water from the separator caused silica gel to get wet. As a response, production operation was paused to renew silica gel. Gas production stage took 3 days by an intermittent manner. After production completed, the results of flow meter data showed that cumulative gas produced amount was more than what was injected into the cell. To find the reason of discrepancy, calibration of the gas flowmeter was checked and

found that it was affected during the experiment, most probably due to moisture. It was decided not to interpret the gas production data due to malfunction of gas flowmeter and only hydrate formation stage of Experiment-1 is discussed.

5.2 EXPERIMENT 2

Experiment-2 took 3 weeks to complete hydrate formation and gas production stages (Figure 5.4). 2.57 moles of methane gas has been injected into high-pressure cell at 71.75 bar-g and 6.07 °C (Figure 5.5). There is a discontinuity of data between days 10 and 13 because of malfunction of data recorder-1 (Figure 5.4).

Figure 5.6 shows pressure decline rate plot of Experiment-2. There a sharp decline in decline rate of pressure at the initial stage which is indicated as Stage-1. After having a sharp decline, almost a linear decline rate is observed (Stage-2) which is followed by a shift to a higher value of decline but a similar trend of the previous stage (Stage-3). The time of the shift corresponds to change in pressure after 5 days (Figure 5.4). When the linear trend of Stage-2 and Stage-3 are compared, it is seen that they are parallel to each other. Although hydrate formation has the highest rate in the 1st stage comparing to the 2nd and the 3rd stages, formation process did not stop and continued in the last 2 stages with very similar rates.

In order to prevent overflow of water due to excessive water production, a low production rate is applied in Experiment-2 which resulted with a very low gas flow rate (lower than 0.1 L/min). Unfortunately, the flow rate is not sensitive to such a low flow rate which was recorded as zero in the data recorder. That is why the gas production stage of Experiment-2 was not interpreted.

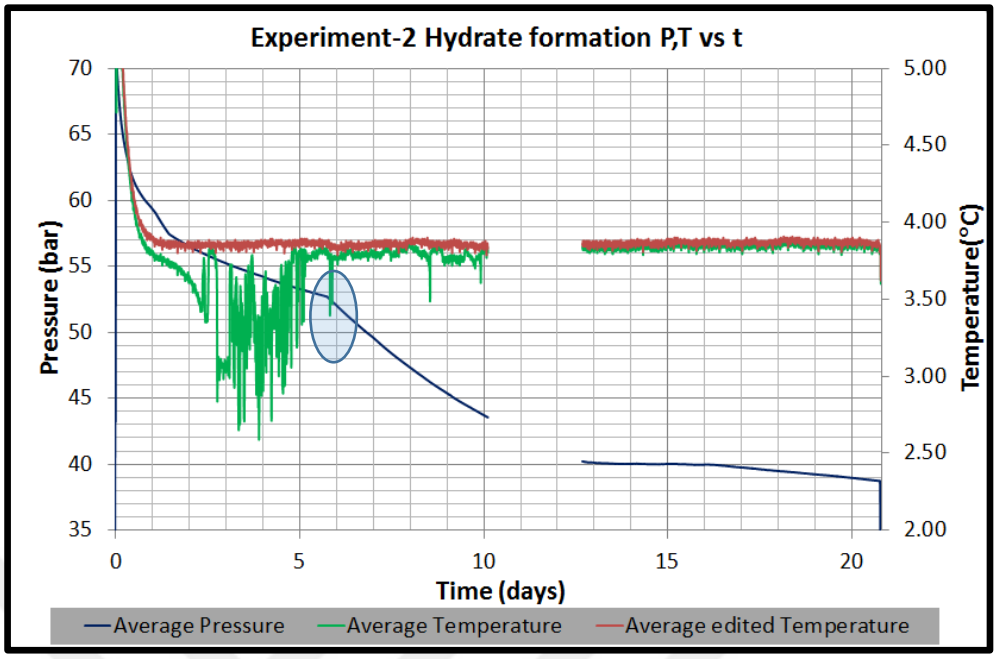

Figure 5.4. Pressure and temperature data of Experiment-2 by time

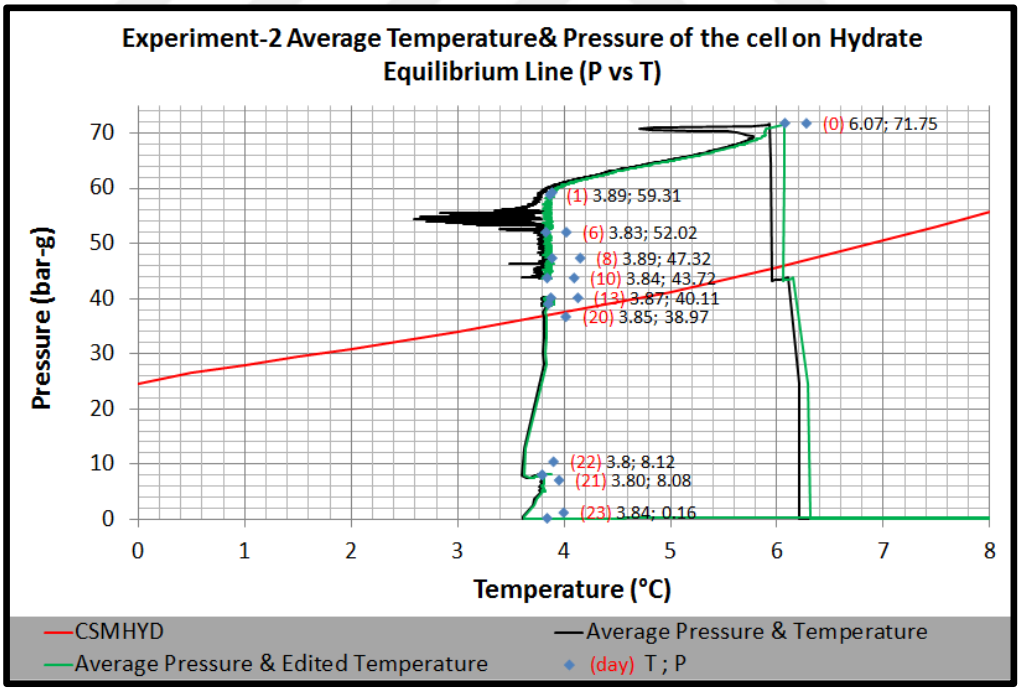

Figure 5.5 Pressure – temperature traverse during hydrate formation and gas production stages in Experiment-2

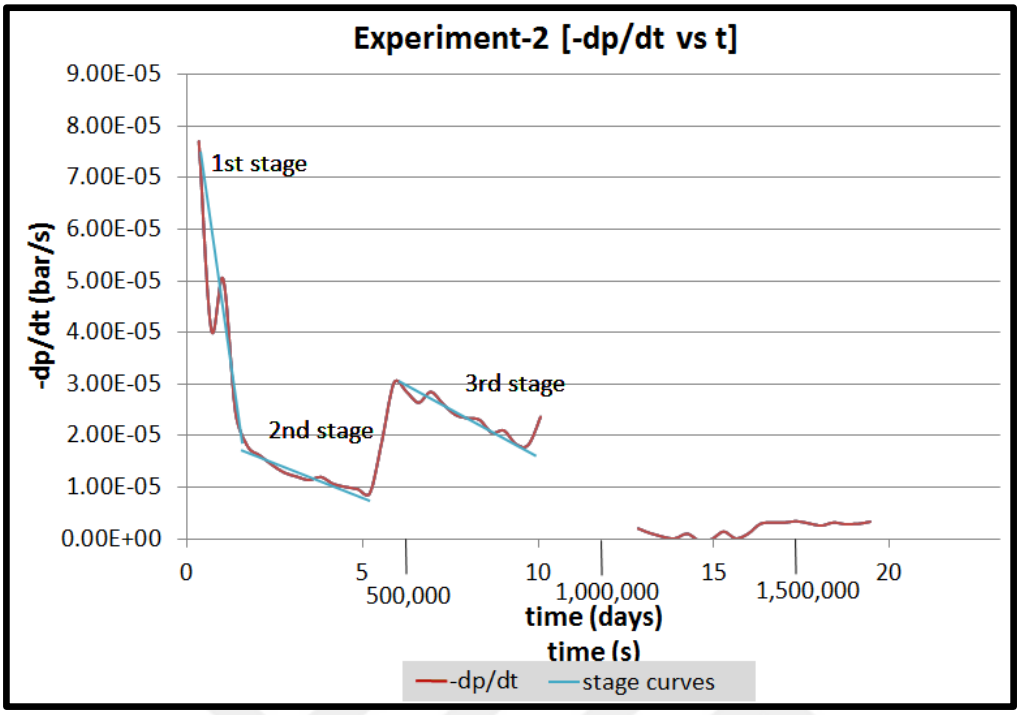

Figure 5.6. Pressure decline rate during hydrate formation of Experiment-2

5.3 EXPERIMENT 3

In the third experiment, hydrate formation process lasted about 3 months. 3.04 moles of methane has been injected at 76.54 bar-g and 19.35 °C. Figure 5.7 shows the pressure-temperature data during hydrate formation period. As indicated there exist two periods (Stage-a and Stage-b) in which sudden pressure drops observed. Figure 5.8 and Figure 5.9 show these two periods in detail. In stage-a, there exist small temperature increase corresponding to pressure drops as an indicator of exothermic reaction of hydrate formation (Figure 5.8). On the other hand, the pressure drops in Stage-b are actually a response of the physical change in the position of hydrate cell by the research team. It was decided to make the cell upside down and return it back into original position in order create an agitation within the cell and it worked well with a sudden pressure response. This small agitation triggered the hydrate formation and resulted with higher gas consumption (Figure 5.10). Although hydrate formation is known as an exothermic process, noticeable

temperature increase in the cell was not observed during the hydrate formation at Stage-b. It might be the amount of the heat produced from the hydrate formation was not high enough to meet with temperature values of conditions supplied from the constant temperature room.

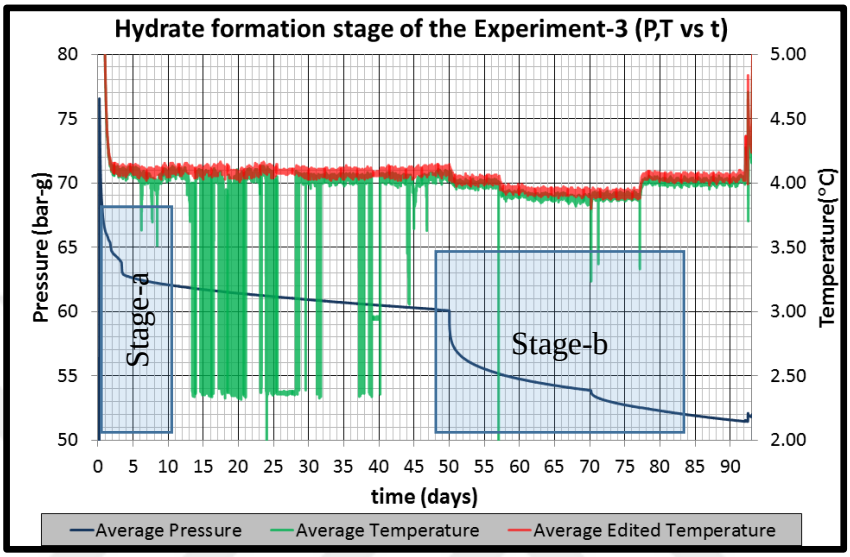

Figure 5.7. Pressure and temperature data of Experiment-3 during hydrate formation

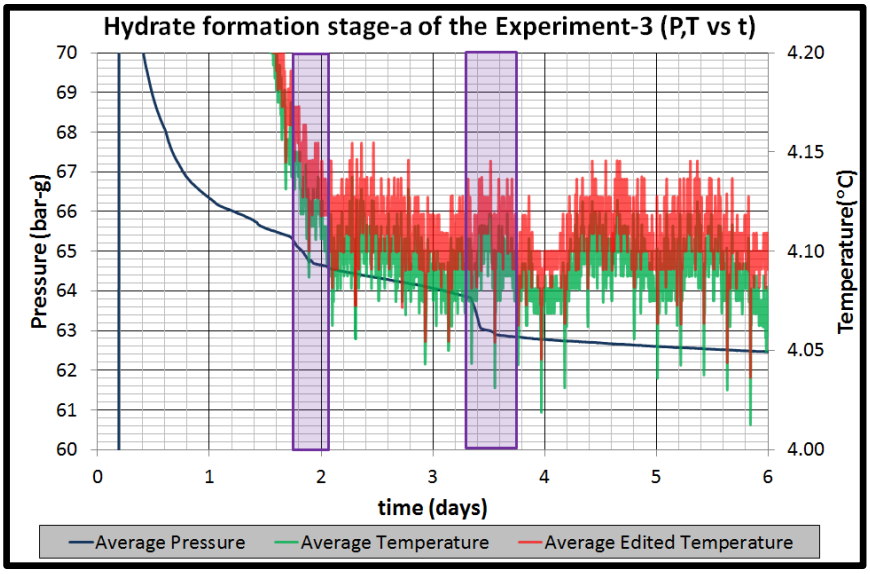

Figure 5.8. Pressure and temperature data of Experiment-3 during hydrate formation (Stage-a)

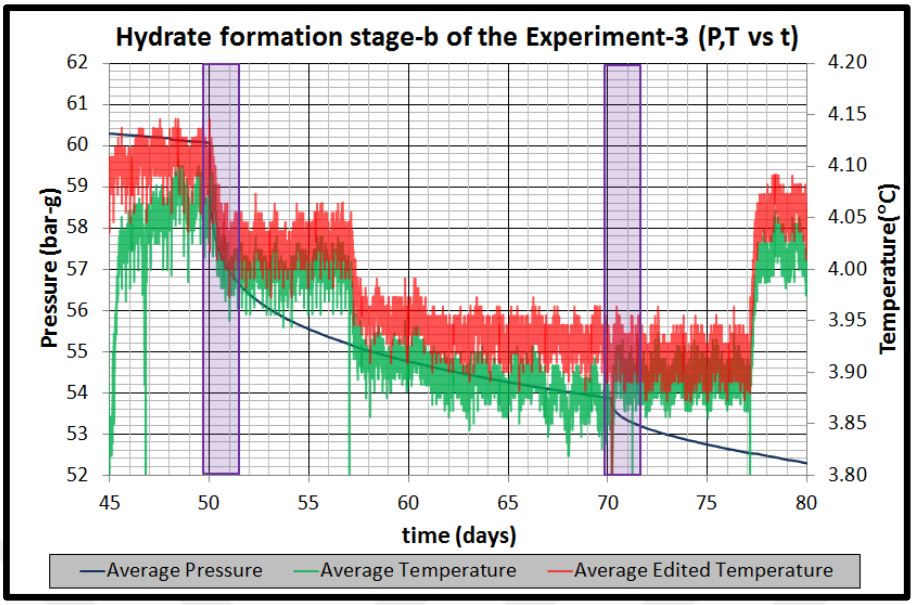

Figure 5.9. Pressure and temperature data of Experiment-3 during hydrate formation (Stage-b)

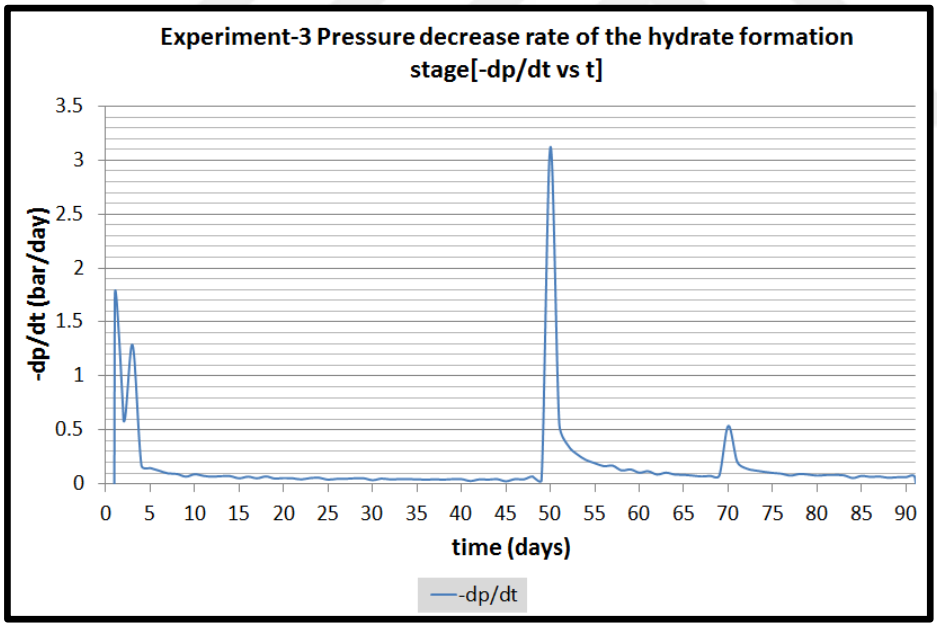

Figure 5.10. Pressure decline rate during hydrate formation of Experiment-3

Another very useful plot for the interpretation of experimental data is the moles of free gas versus time plot. Figure 5.11 gives the moles of free gas and gas consumption rate versus time plot of the same data given in Figures 5.7. This plot is obtained after processing the experimental temperature and pressure data with the use of real gas law (Equation 5.1).

$$PV = ZnRT \qquad (5.1)$$

where ;

P: Pressure (psia)

V: Volume (ft^3)

Z: Gas compressibility factor

n: Number of moles (lb-mole)

R: Universal gas constant (10.73 psia ft^3/lb-mole°R)

T: Temperature (°R)

Variables P and T of Equation 5.1 are the recorded data. Gas compressibility factor of methane (z) is calculated by using Lee and Kesler's (1975) compressibility factor expression. Free gas volume is assumed constant during hydrate formation. Free gas mole graph exhibit a resemblance with pressure change since the temperature change is very limited throughout the test. On the other hand, a sudden and high change in pressure corresponds higher rate of gas consumption or higher rate of hydrate formation.

At the end of hydrate formation period, when cell pressure was 51.44 bar-g, it was decided to start gas production stage. In order to achieve the hydrate dissociation warm water circulation was started through spiral pipe which enables the circulation around the artificial well in the cell. The circulation temperature is fixed to constant temperature value of 20 °C. A low circulation rate of warm water increased the temperature around the artificial well around 10 °C in one day. A

slight increase in cell temperature resulted with an increase in pressure to the average value of the 51.82 bar-g just before the production started (Figure 5.12).

Data collected during gas production stage of Experiment-3 is presented in Figure 5.13: This data includes average temperature, average pressure, wellhead pressure (or set pressure of back-pressure regulator), gas flow rate and cumulative water production as function of time. The following observations are made from this data:

1. At first there is no gas flow but small amount of water production due to expansion of compressed water which enters into the artificial well. During this period, no gas was able to reach into the wellbore since the free gas water interface was at a higher position than the perforations depth.
2. On the other hand, average cell pressure was higher than the wellhead pressure which was actually due to compressed free gas at the top of cell.
3. Later, an increase in water production was observed with no or very little gas flow. This is attributed as the gas locking effect due to very high saturation of water in the porous media which hinders the flow of gas as a result of relative permeability.
4. At about 1000 sec of production stage a clear indication of temperature decrease is observed which is a sign of hydrate dissociation due to endothermic nature of dissociation.
5. Later intermittent nature of gas production with higher rate of water production is experienced until water production minimized.
6. The highest gas flow was observed when water flow became very low.

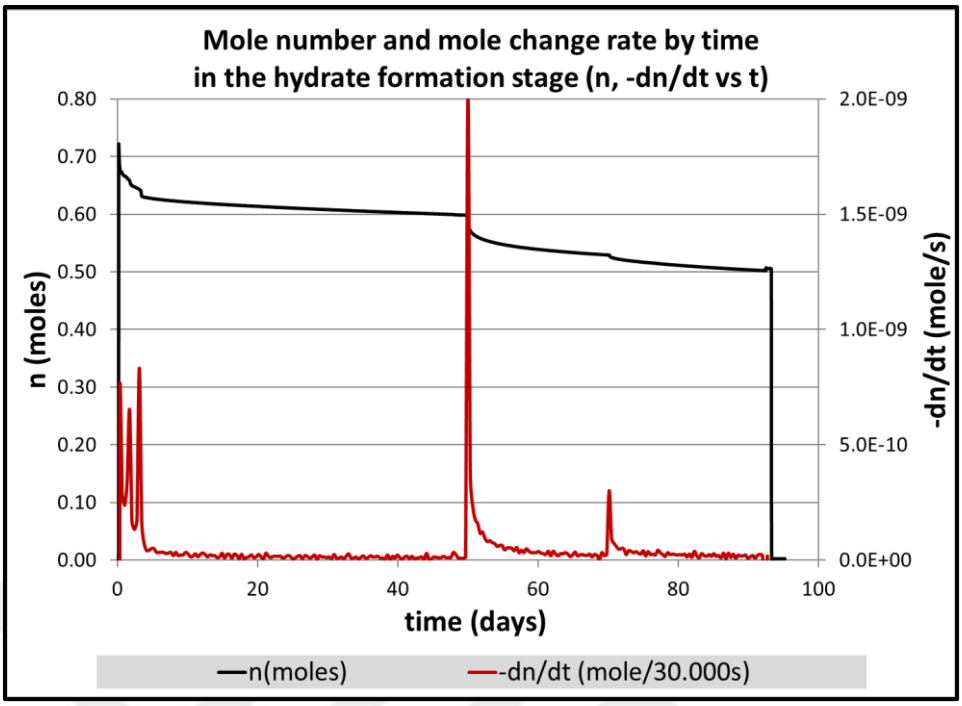

Figure 5.11. Change in moles of free gas and gas consumption rate during hydrate formation in Experiment-3

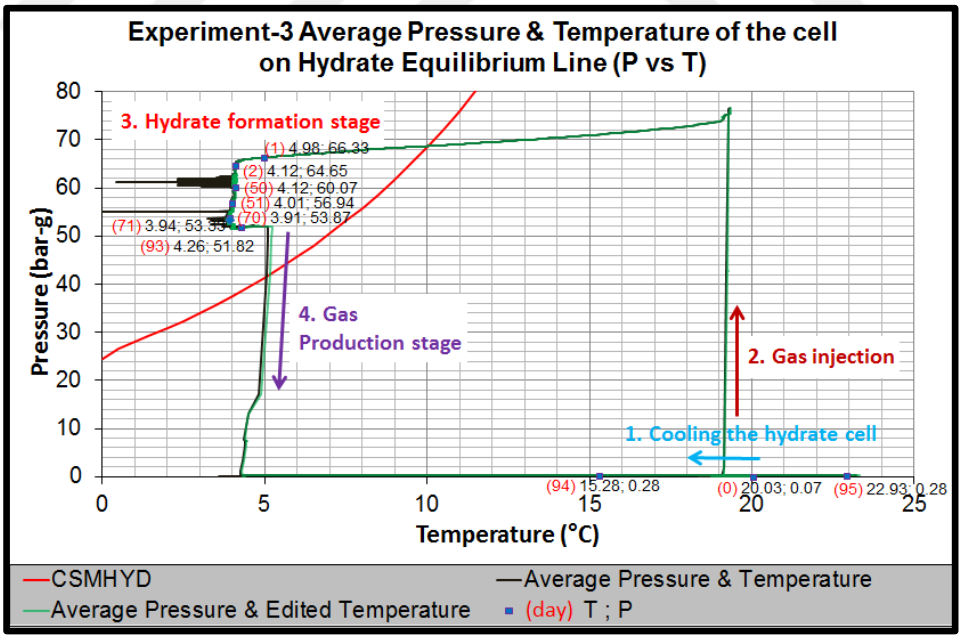

Figure 5.12. Pressure – temperature traverse during hydrate formation and gas production stages in Experiment-3

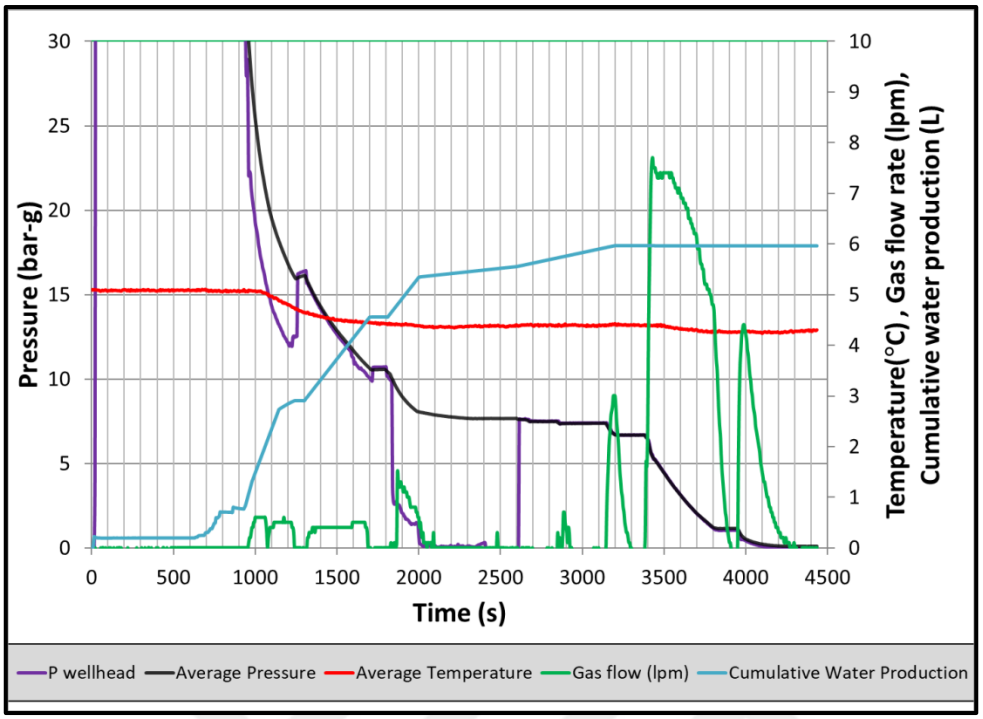

Figure 5.13. Experiment production stage (Pressure, Temperature, Gas Flow Rate, Cumulative water production vs time)

Figure 5.14. shows temperature distributions at different depths in the cell based on average temperature values of TCs with different lengths. As observed the deeper the layer in the cell from top cover the less the temperature changes during dissociation / gas production. On the other hand, the top layer (60 mm from the top cover) had the highest cooling due to hydrate dissociation. There is about 2 °C drop in temperature after 1000 sec which was the time for the initiation of dissociation. This can be interpreted that most of hydrates formed closer to top cover or closer to water – gas interface.

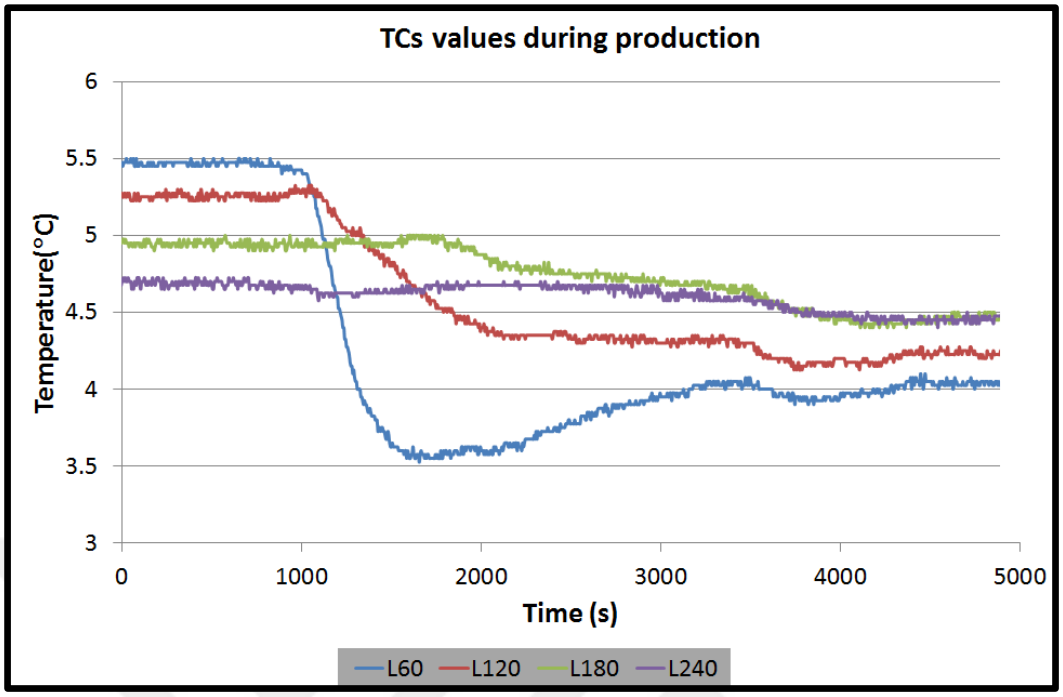

Figure 5.14. Experiment-3 thermocouple values in different depths during production

In order to understand the location of the hydrate by looking the possible temperature changes in the cell, a 3D open source software called “Paraview” has been used to illustrate temperature distributions in the cylindrical high pressure hydrate cell. First, the grid has been constructed and 27 000 points have been defined to create a cube (30x30x30 points). Corresponding temperature values coming from 16 TCs for each point have been calculated through “Matlab” by scattered interpolation of the 16 TCs values and then animation views have been exported for every 36 000 seconds (10 hours). It has been seen that hydrate formed not only in one specific place but in the layers above 6 cm depths from the top cover. The dissociation observed with the temperature drop in the depths of 6 cm from the top cover as a result of endothermic process of hydrate dissociation. Temperature distribution layers are available in the Appendix.

CHAPTER 6

CONCLUSION

Interpretation of hydrate formation and gas production data of three experiments of this study reveal the following conclusions.

1. Hydrate formation in porous media with no agitation is possible but takes very long. It could be increased by continuous circulation of high pressure gas.
2. Thermal stimulation along with depressurization is a better production scheme compared to depressurization alone since dissociation is an endothermic process which may cause a secondary hydrate formation or icing.
3. Gas flow is hindered, initially, by high flow rate of water. It is attributed to the higher saturation of water in porous media which exhibits higher relative permeability of water. In addition, higher flow rate of water may block the flow of water in wellbore. This brings the question how to control the water production after dissociation.

REFERENCES

Abbasov, A., Merey, Ş., Parlaktuna, M., (2016), "Experimental investigation of carbon dioxide injection effects on methane-propane-carbon dioxide mixture hydrates", Journal of Natural Gas Science and Engineering, 34, 1148 – 1158

Ahmed, U., & Meehan, D. N. (2016). Unconventional oil and gas resources: exploitation and development (pp. 3-7). Boca Raton, FL: CRC Press.

Bai, Y., Li, Q., Li, X. et al. Numerical simulation on gas production from a hydrate reservoir underlain by a free gas zone. Chin. Sci. Bull. 54, 865–872 (2009) doi:10.1007/s11434-008-0575-z

Borden, K. 2014. Flow Assurance: Hydrates and Paraffin Management. Society of Petroleum Engineers. doi:10.2118/0214-0029-OGF.

Cheng, C., Zhao, J., Yang, M., Liu, W., Wang, B., Song, Y., (2014), "Evaluation of Gas Production from Methane Hydrate Sediments with Heat Transfer from Over-Underburden Layers", Energy and Fuels, 29, 1028 – 1039.

Dolf Gielen, Francisco Boshell, Deger Saygin, Morgan D. Bazilian, Nicholas Wagner, Ricardo Gorini, The role of renewable energy in the global energy transformation, Energy Strategy Reviews, Volume 24, 2019, Pages 38-50, ISSN 2211-467X, https://doi.org/10.1016/j.esr.2019.01.006.

Du, Y., Feng, Z., (2010) "Experimental Studies of Natural Gas Hydrate Dissociation in Porous Media by Inhibitor Injection with the 2D Experimental System", Proceedings of the Twentieth (2010) International Offshore and Polar Engineering Conference, Beijing, China, June 20 -25

Feng, J-C., Wang, Y., Li, X-S., Li, G., Zhang, Y., (2015), "Three dimensional experimental and numerical investigations into hydrate dissociation in sandy reservoir with dual horizontal wells", Energy, 90, 836 – 845

Fitzgerald, G.C., Castaldi, M.J., (2013), "Thermal Stimulation Based Methane Production from Hydrate Bearing Quartz Sediment", Ind. Eng. Chem. Res., 52, 6571 – 6581.

Holditch, S.A.: "Tight gas sands", SPE J. Pet. Technol. 58, 2006

Koh, C. A., Sum, A.K., Sloan, D.E. 2009. Gas hydrates: Unlocking the energy from icy cages. Journal of Applied Physics. doi:10.1063/1.3216463

Konno, Y., Jin, Y., Shinjou, K., Nagao, J., (2014), "Experimental evaluation of the gas recovery factor of methane hydrate in sandy sediment", RSC Adv., 4, 51666 – 51675

Lee B.I., Kesler M.G., "A Generaliezed Thermodynamic Correlation Based on Three-Parameter Corresponding States", AIChE J., 21, pp. 510-527, (1975).

Lee, Joo & Ryu, Byong-Jae & Yun, Tae & Lee, Jaehyung & Cho, Gye-Chun. (2011). Review on the Gas Hydrate Development and Production as a New Energy Resource. KSCE Journal of Civil Engineering. 15. 689-696. 10.1007/s12205-011-0009-3.

Li, G., Li, B., Li, X-S., Zhang, Y., Wang, Y., (2012) "Experimental and Numerical Studies on Gas Production from Methane Hydrate in Porous Media by Depressurization in Pilot-Scale Hydrate Simulator", Energy & Fuels, 26, 6300 – 6310.

Li, B., Li, X-S., Li, G., (2014), "Kinetic studies of methane hydrate formation in porous media based on experiments in a pilot-scale hydrate simulator and a new model", Chemical Engineering Science, 105, 220 – 230.

Linga, P., Haligva, C., Nam, S.C., Ripmeester, J.A., Englezos, P., (2009) "Recovery of Methane from Hydrate Formed in a Variable Volume Bed of Silica Sand Particles", Energy & Fuels, 23, 5508–5516.

Liu, C., Sun, J., Ye, Y., (2013) "Chapter 11- Experimental Studies on Techniques to Extract Natural Gas Hydrate", Ed: Ye, Y., Liu, C., Natural Gas Hydrates - Experimental Techniques and Their Applications, Springer-Verlag, Berlin Heidelberg.

Merey, Ş. & Longinos, S. N. (2019). The gas hydrate potential of the Eastern Mediterranean basin. Bulletin of the Mineral Research and Exploration, 160 (160) , 117-134 . DOI: 10.19111/bulletinofmre.502275

Moridis, G.J., Collett, T.S., (2003) "Strategies for Gas Production from Hydrate Accumulations Under Various Geologic Conditions", Report LBNL-52568, Lawrence Berkeley National Laboratory, Berkeley, California.

Moridis, George & Kowalsky, M. & Pruess, Karsten. (2007). Depressurization-Induced Gas Production From Class1 Hydrate Deposits. SPE Reservoir Evaluation & Engineering - SPE RESERV EVAL ENG. 10. 458-481. 10.2118/97266-PA.

Nair, V.C., Ramesh, S., Ramadass, G.A., Sangwai, J.S., (2016) "Influence of thermal stimulation on the methane hydrate dissociation in porous media under confined reservoir", Journal of Petroleum Science and Engineering, 147, 547 – 559

Ors, O., Sınayuç, Ç., (2014) "An experimental study on the CO2–CH4 swap process between gaseous CO2 and CH4 hydrate in porous media", Journal of Petroleum Science and Engineering, 119, 156–162.

Schicks, J., Spangenberg, E., Giese, R., Steinhauer, B., Klump, J., Luzi, M., (2011), "New Approaches for the Production of Hydrocarbons from Hydrate Bearing Sediments", Energies, 4, 151 – 172.

Sloan, E.D. Jr.; Clathrate Hydrates of Natural Gases, Marcel Dekker, NY, 641 pp. 1990

Sloan Jr ED, Koh CA. Clathrate hydrates of the natural gases. 3rd ed. Boca Raton, 9FL: CRC Press; 2008.

Song, Y., Zhang, L., Lv, Q., Yang, M., Ling, Z., Zhao, J., (2016) "Assessment of gas production from natural gas hydrate using depressurization, thermal stimulation and combined methods", RSC Adv, 6, 47357 – 47367.

Sotirios Nik. Longinos, Mahmut Parlaktuna (2021), Kinetic Analysis of Dual Impellers on Methane Hydrate Formation, International Journal of Chemical Reactor Engineering 19(2):155-165, doi.org/10.1515/ijcre-2020-0231

Tang, L.G., Xiao, R., Huang, C., Feng, Z.P., Fan, S., (2005) "Experimental investigation of production behavior of gas hydrate under thermal stimulation in unconsolidated sediment", Energy & Fuels, 19, 2402 – 2407

U.S. Energy Information Administration - EIA - independent statistics and analysis. (2012, November 7). Potential of gas hydrates is great, but practical development is far off. Today in Energy - U.S. Energy Information Administration (EIA).

U.S. Energy Information Administration – EIA "Gas - Fuels & Technologies" (2020, September 16). https://www.iea.org/fuels-and-technologies/gas

Xiong, L., Li, X., Yi Wang, L., Xu, C., (2012) "Experimental Study on Methane Hydrate Dissociation by Depressurization in Porous Sediments", Energies, 5, 518 – 530.

Yang, X., Sun, C-Y., Su, K-H., Yuan, Q., Li, Q-P., Chen, G-J., (2012), "A three-dimensional study on the formation and dissociation of methane hydrate in porous sediment by depressurization", Energy Conversion and Management, 56, 1-7

Yang, X., Sun, C-Y., Yuan, Q., Ma, P-C., Chen, G.J., (2010) "Experimental Study on Gas Production from Methane Hydrate-Bearing Sand by Hot-Water Cyclic Injection", Energy & Fuels, 24, 5912–5920.

APPENDICES

A. Paraview 3-D layered drawings for the Experiment

Every time step represents 36.000 seconds (10 hours). 228 time steps shown;

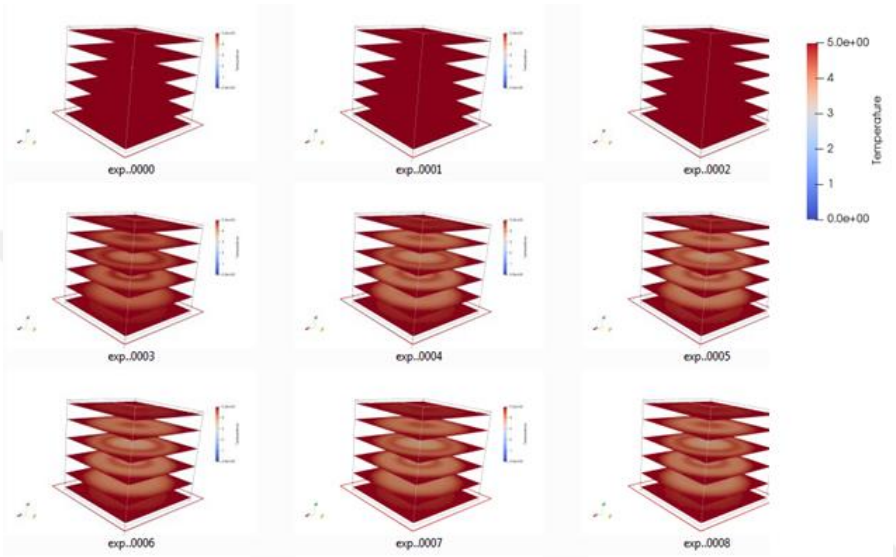

Figure A.1. Time steps of 0-8

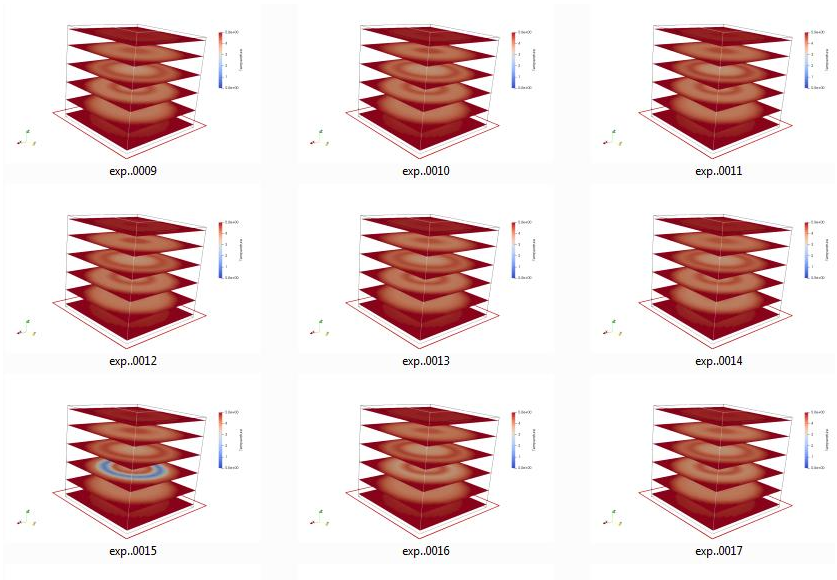

Figure A.2. Time steps of 9-17

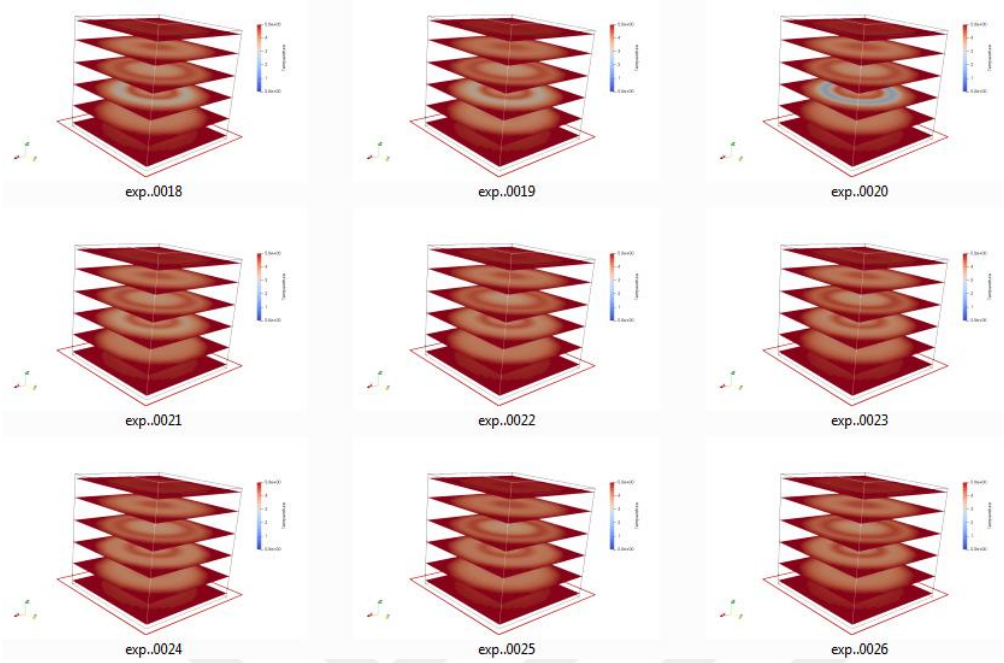

Figure A.3. Time steps of 18-26

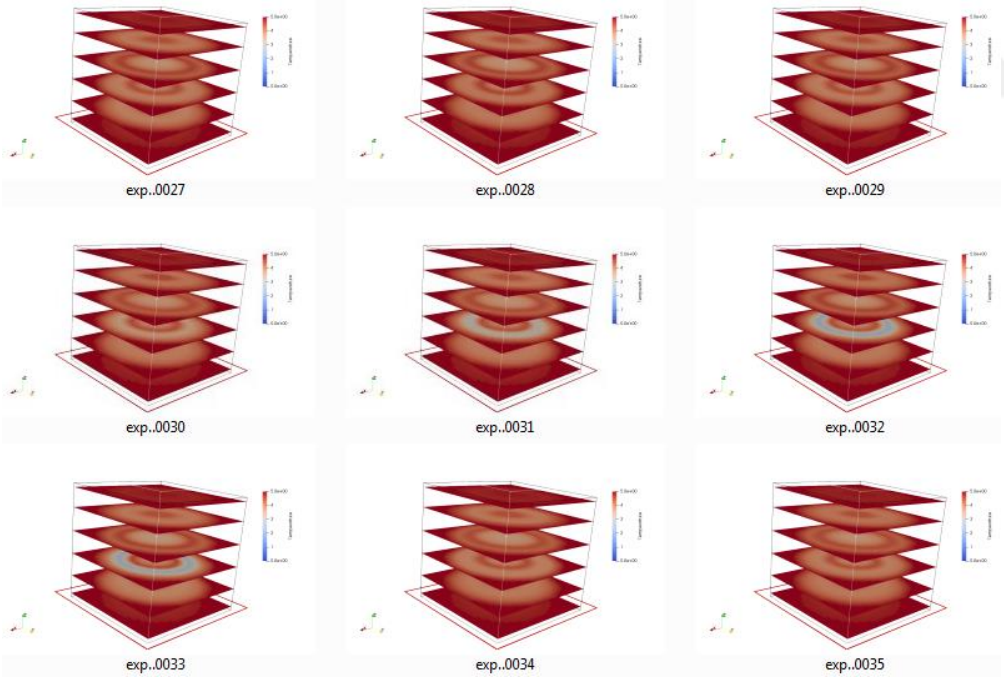

Figure A.4. Time steps of 27-35

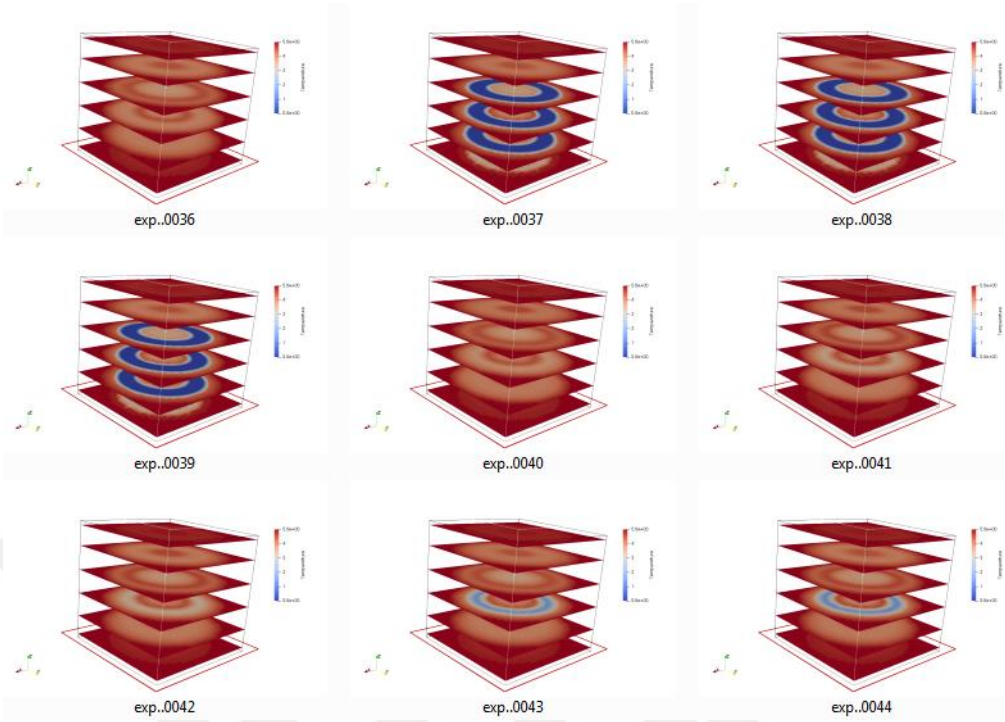

Figure A.5. Time steps of 36-44

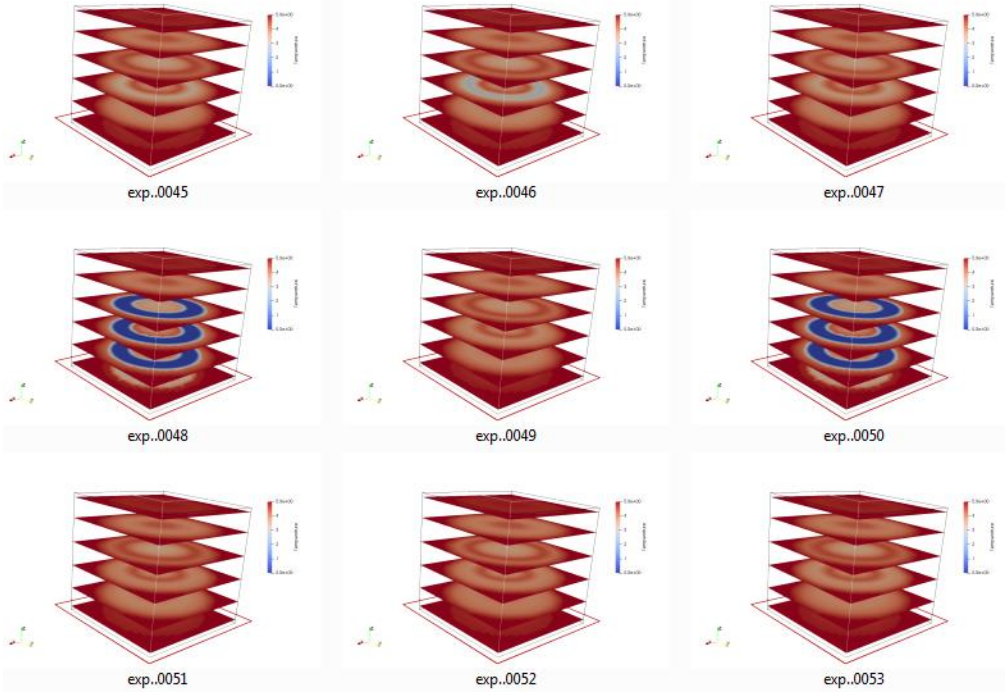

Figure A.6. Time steps of 45-53

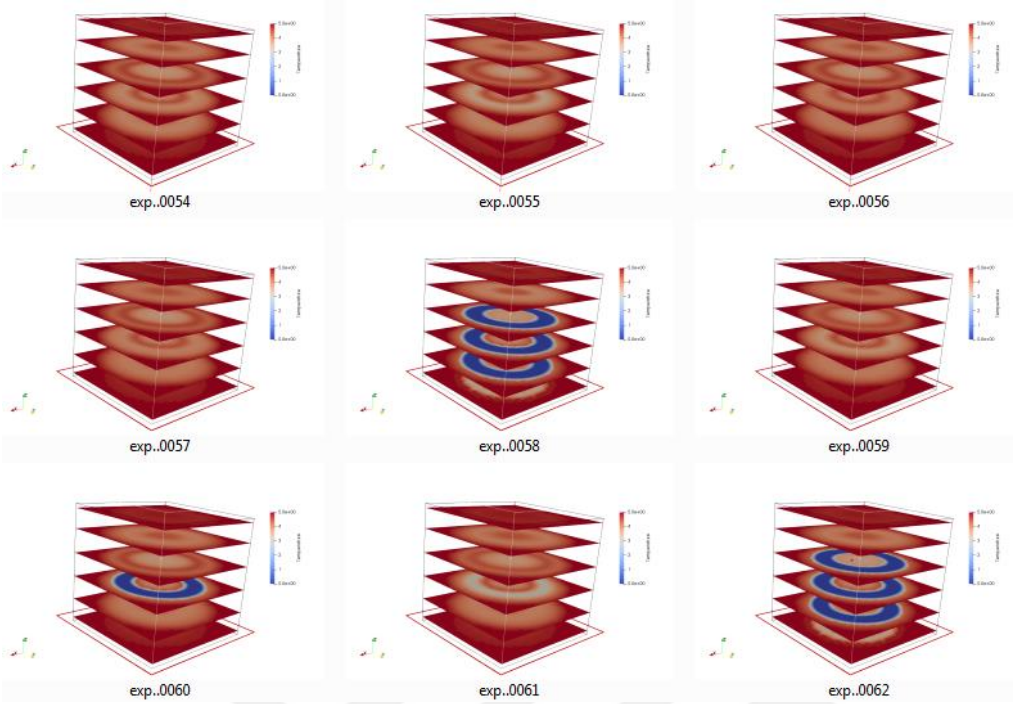

Figure A.7. Time steps of 54-62

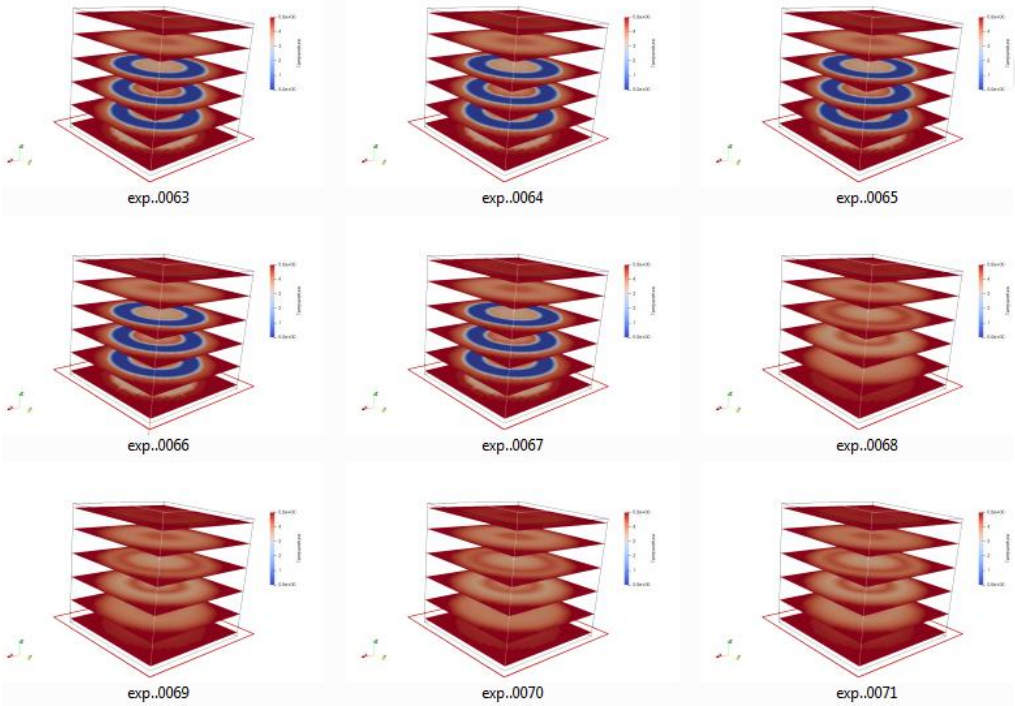

Figure A.8. Time steps of 63-71

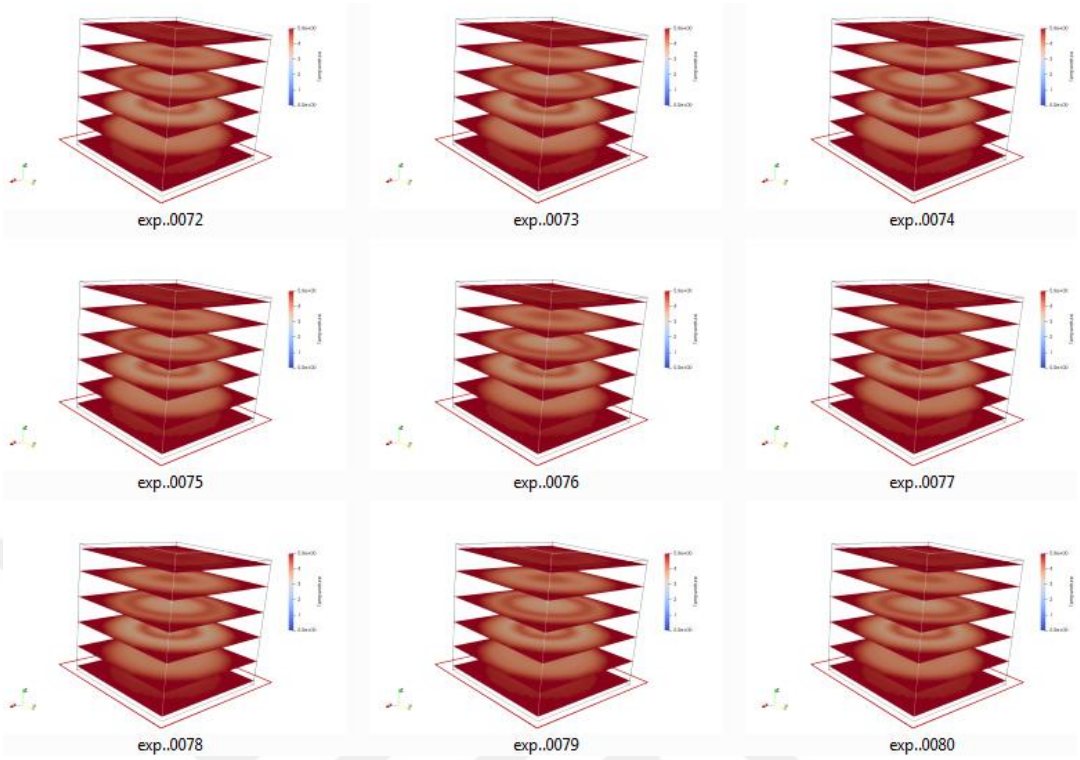

Figure A.9. Time steps of 72-80

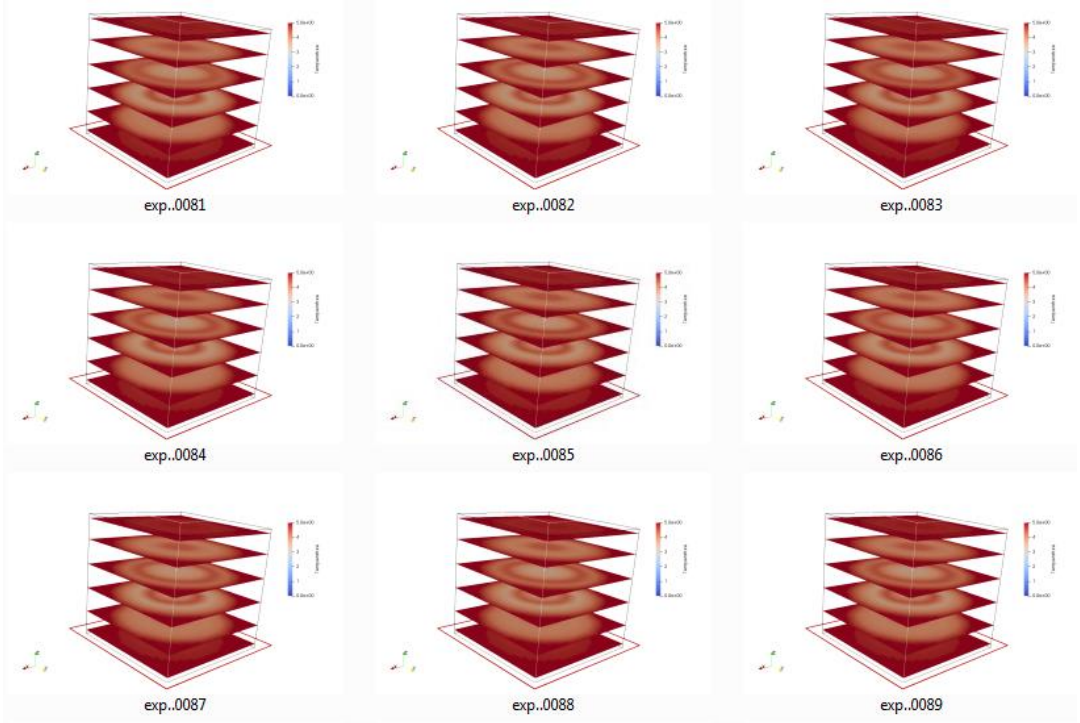

Figure A.10. Time steps of 81-89

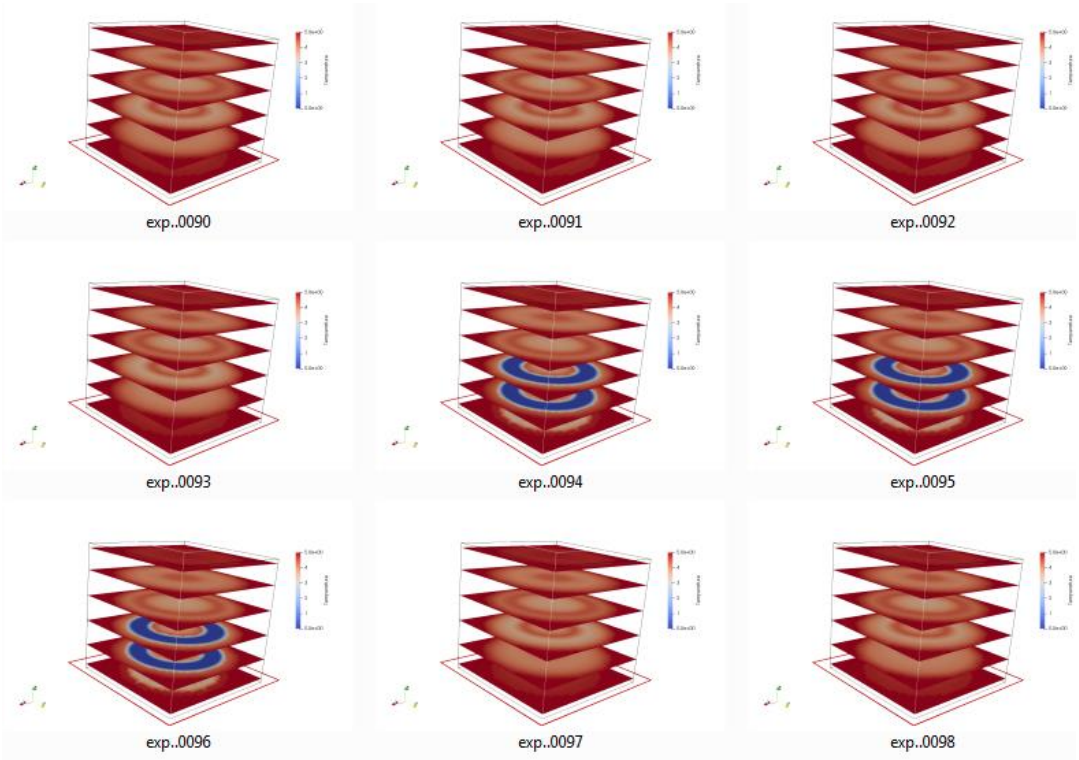

Figure A.11. Time steps of 90-98

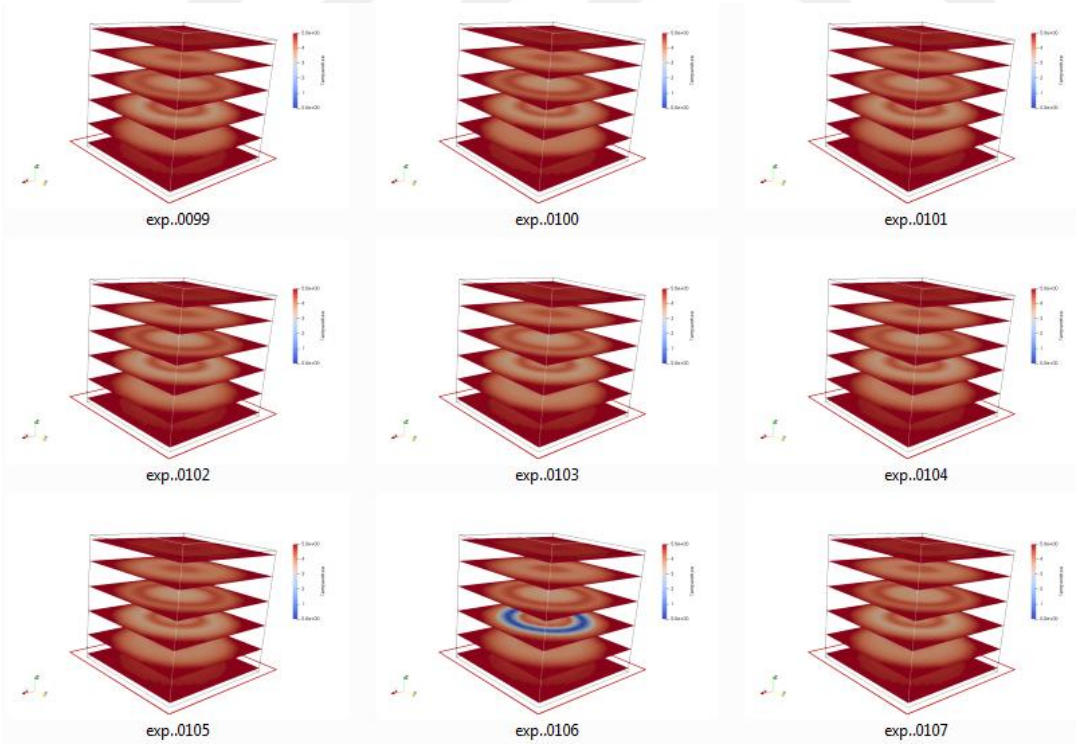

Figure A.12. Time steps of 99-107

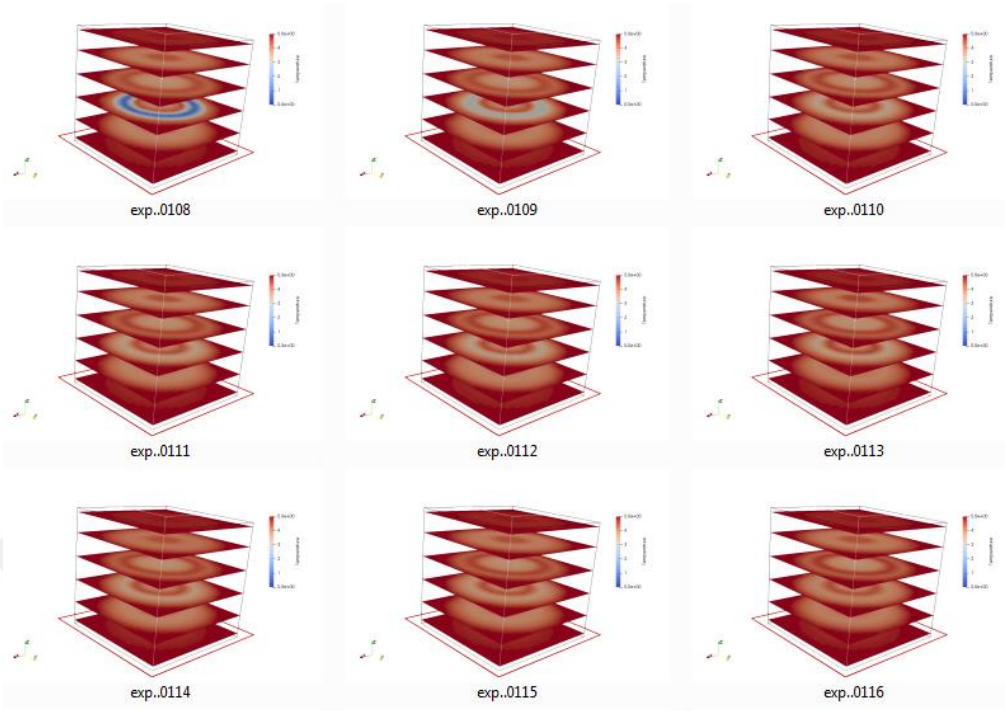

Figure A.13. Time steps of 108-116

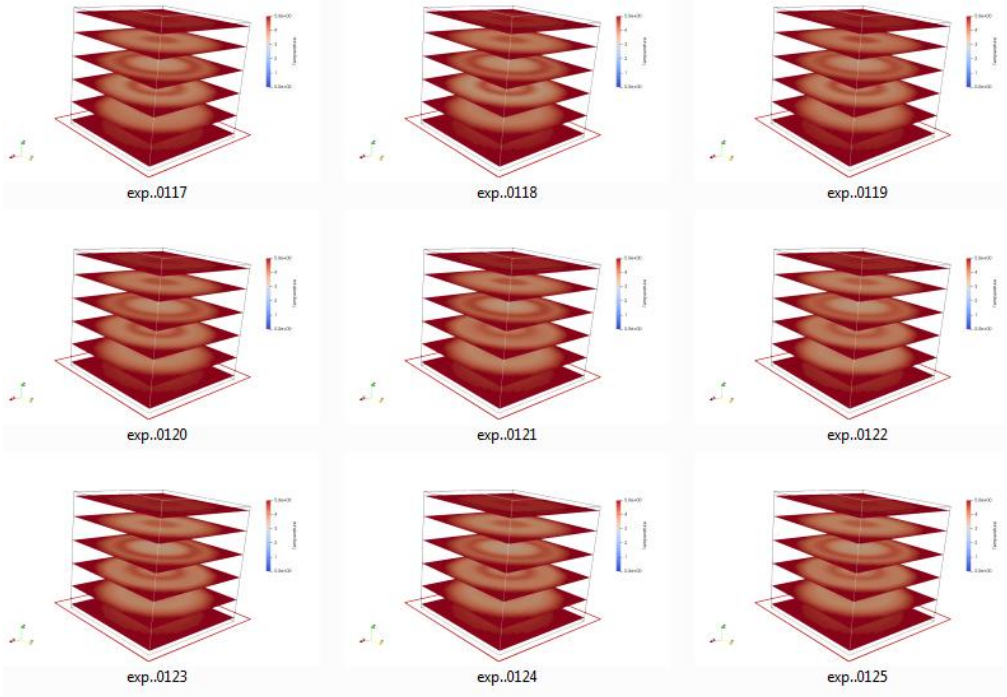

Figure A.14. Time steps of 117-125

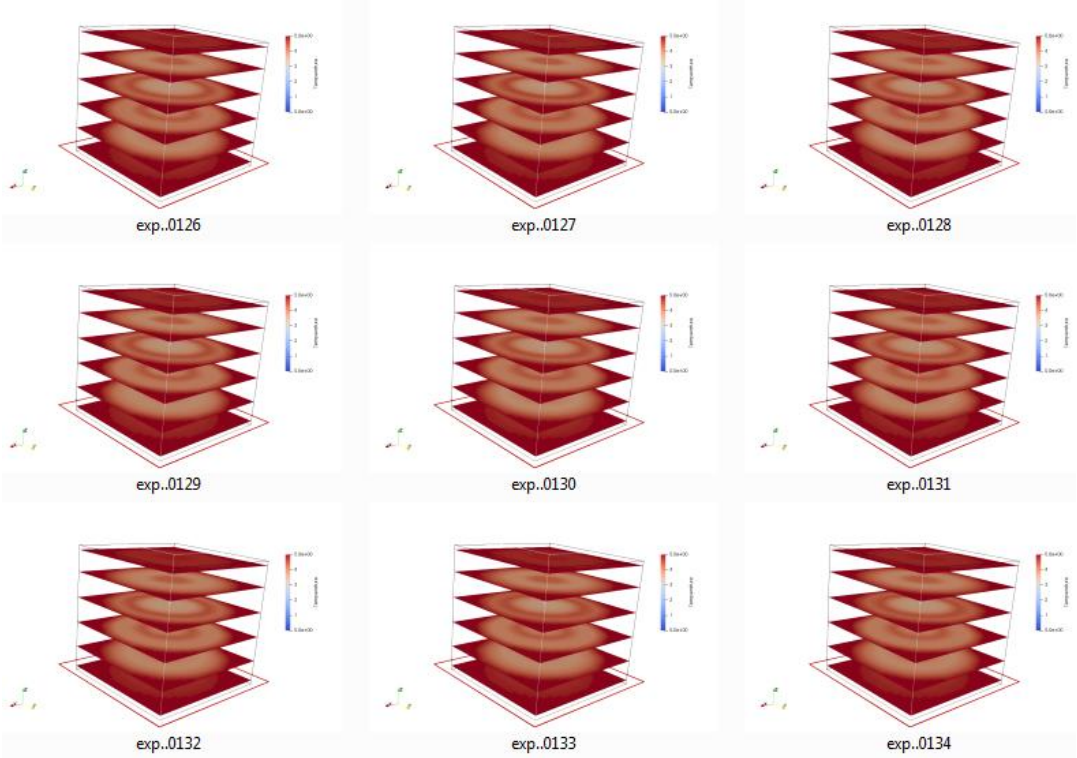

Figure A.15. Time steps of 126-134

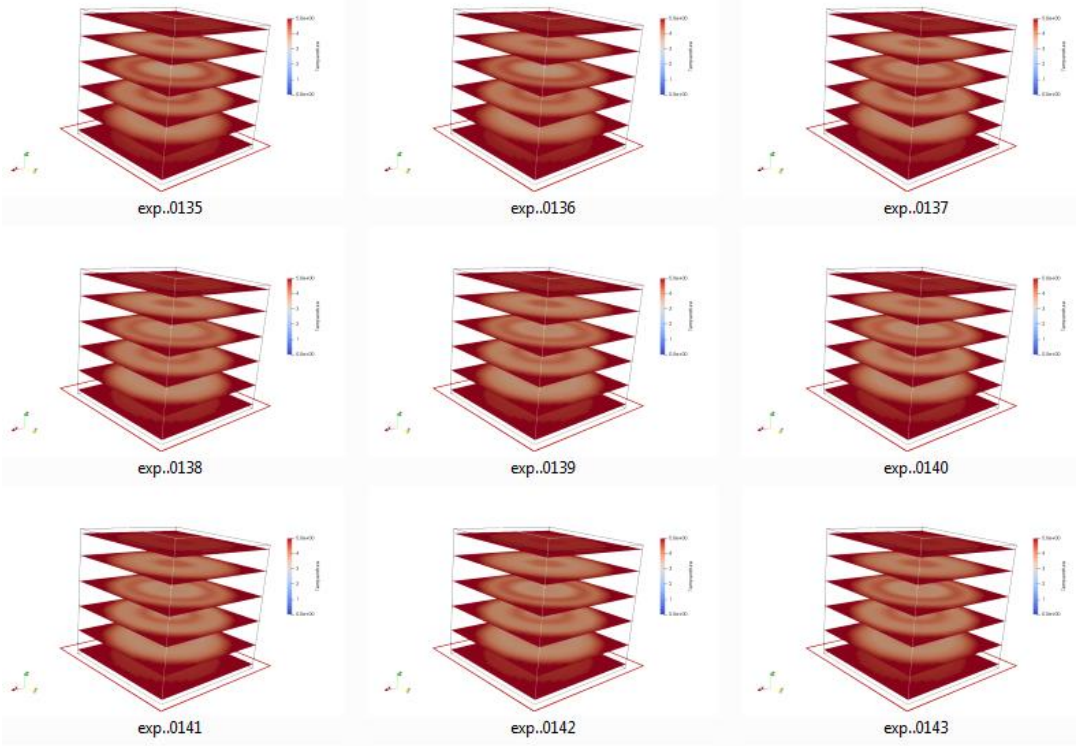

Figure A.16. Time steps of 135-143

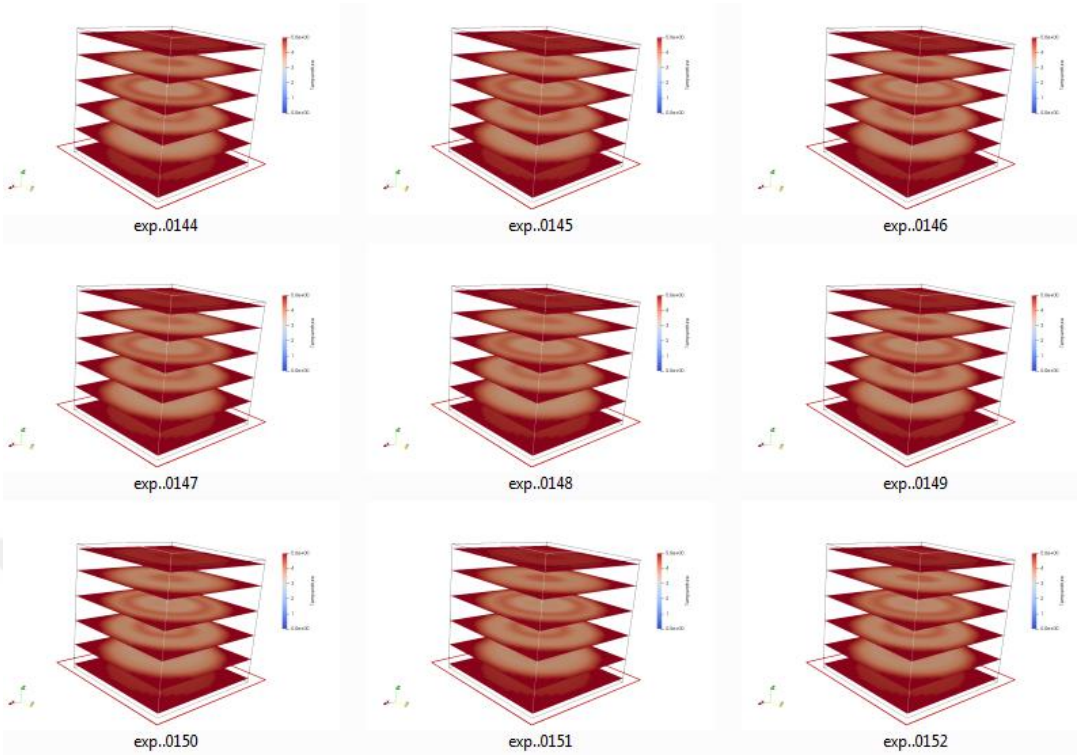

Figure A.17. Time steps of 144-152

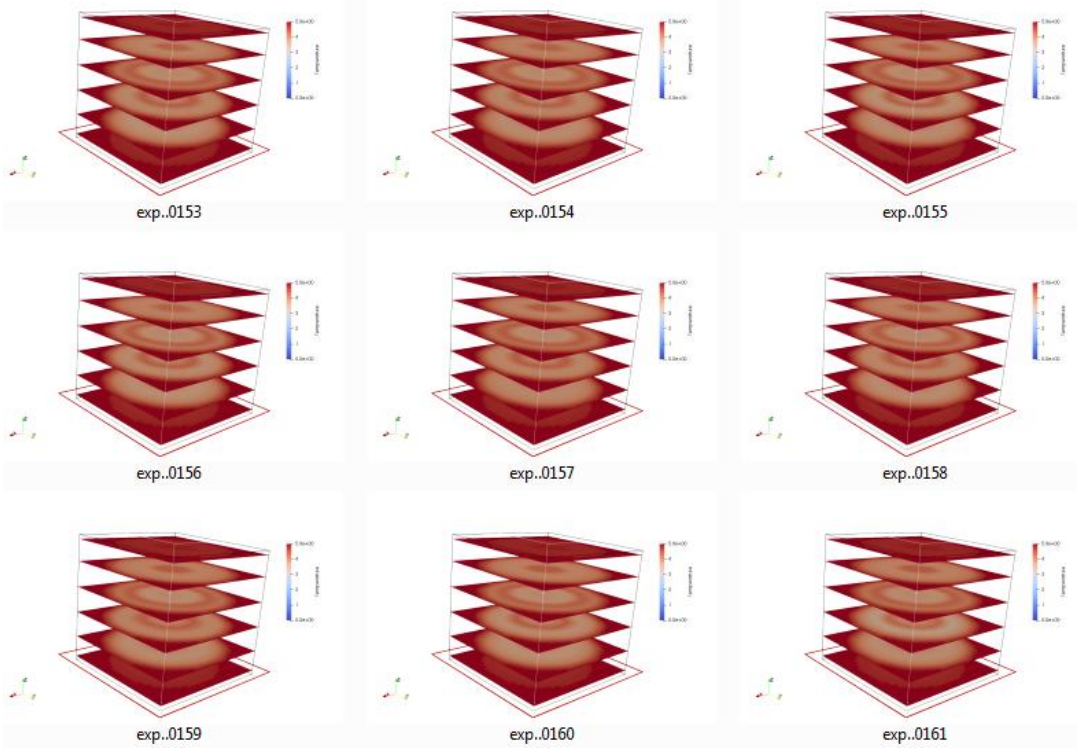

Figure A.18. Time steps of 153-161

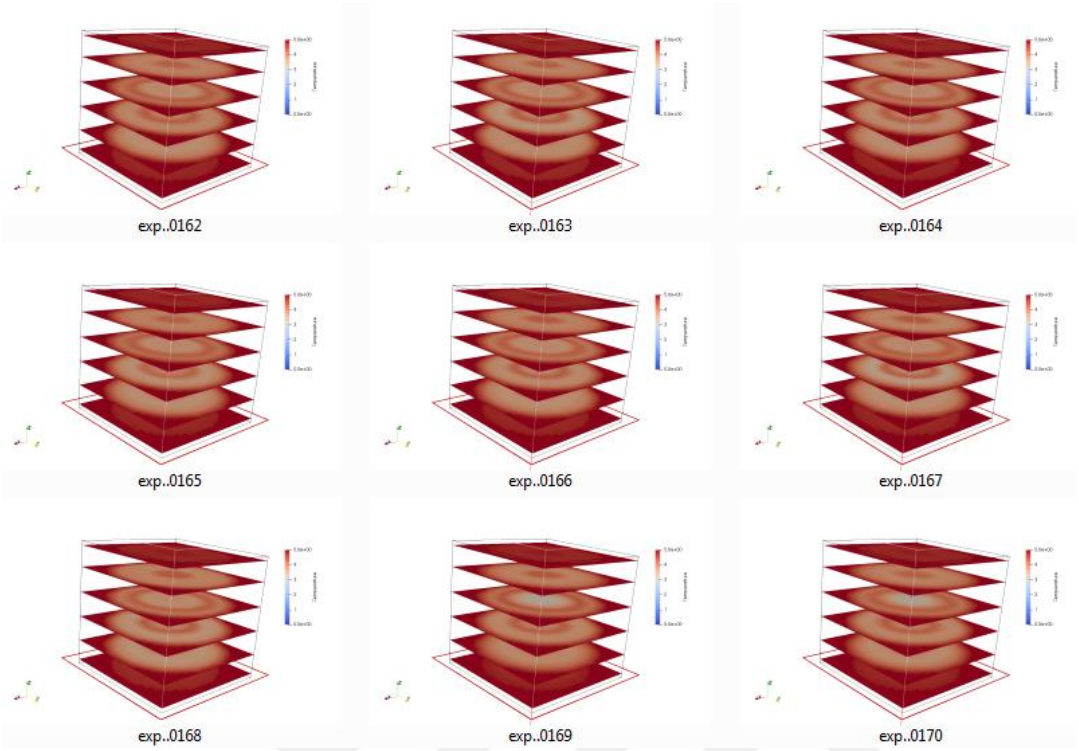

Figure A.19. Time steps of 162-170

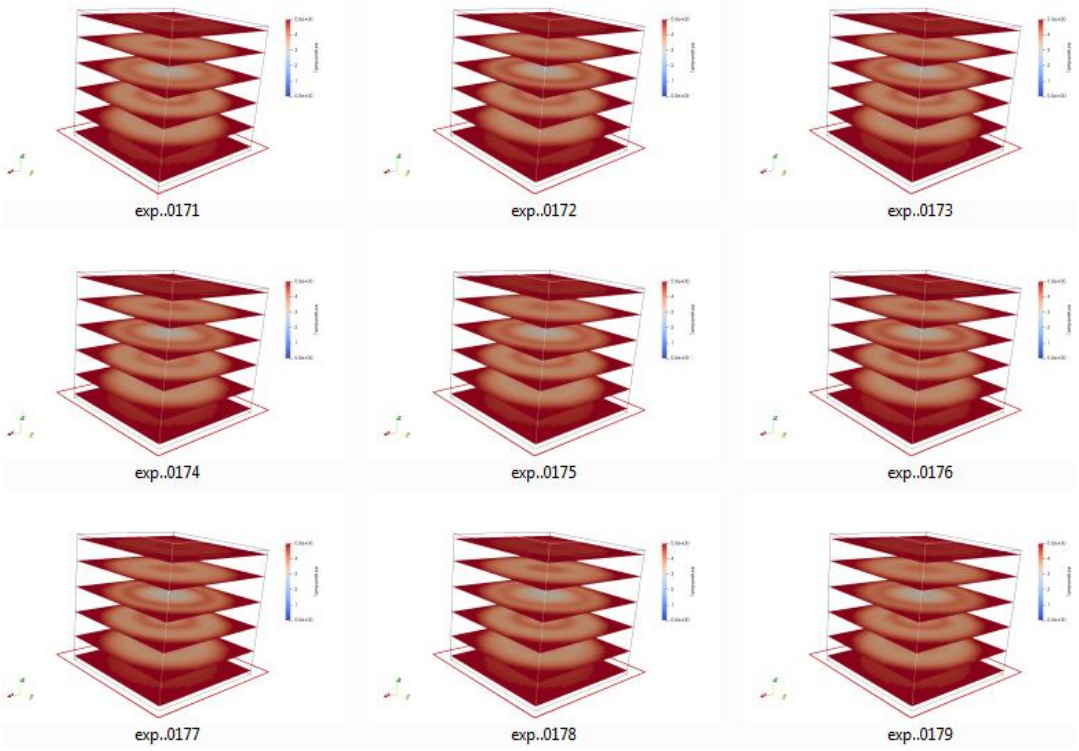

Figure A.20. Time steps of 171-179

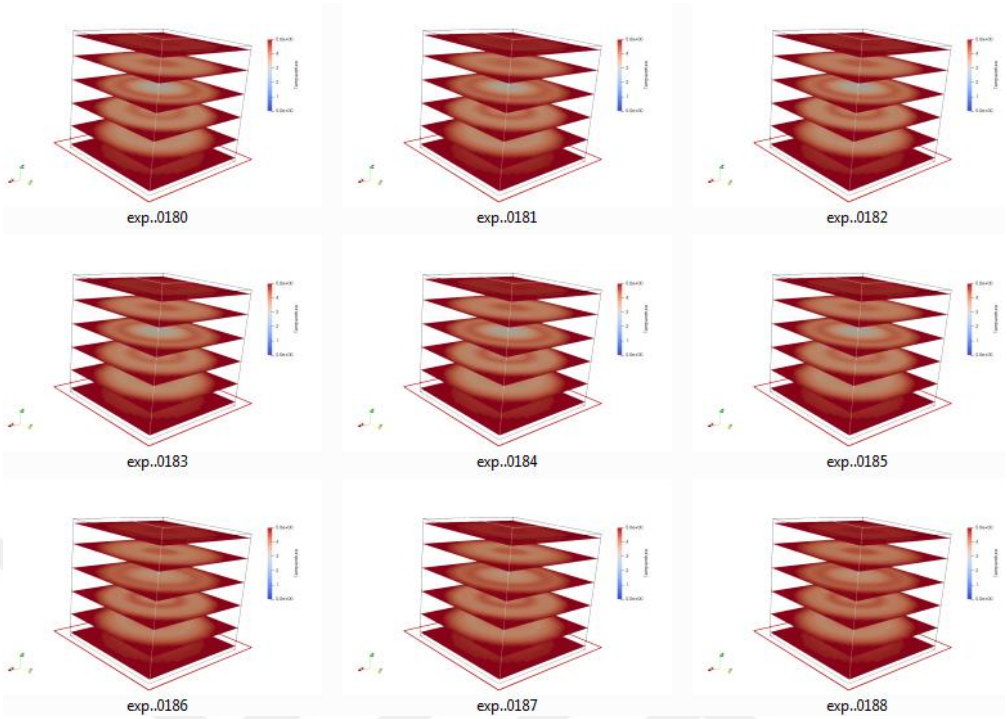

Figure A.21. Time steps of 180-188

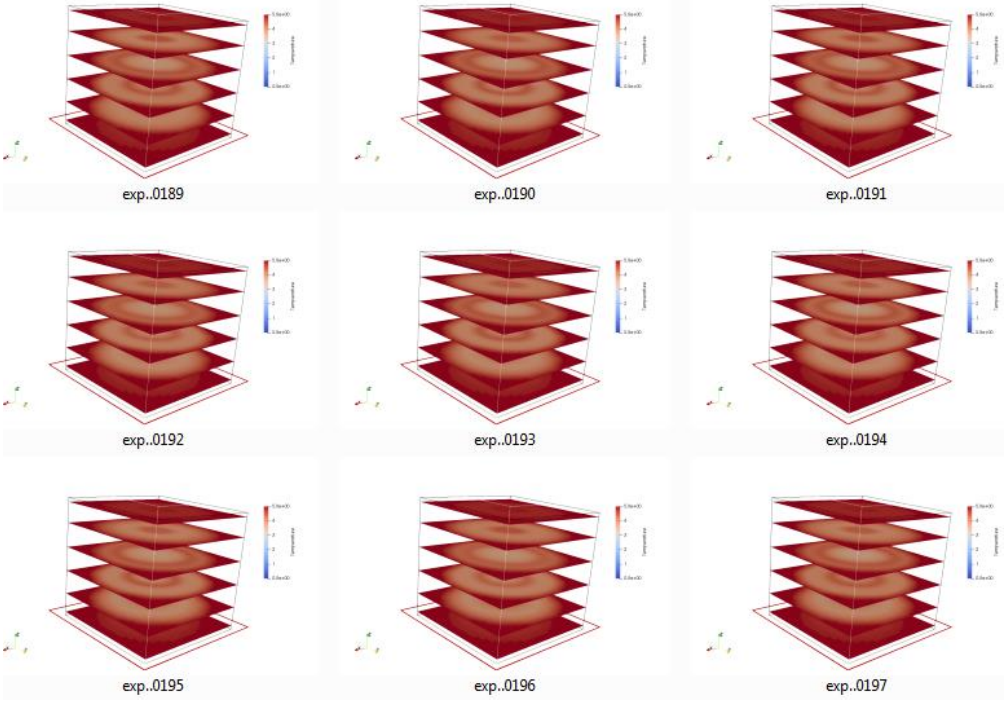

Figure A.22. Time steps of 189-197

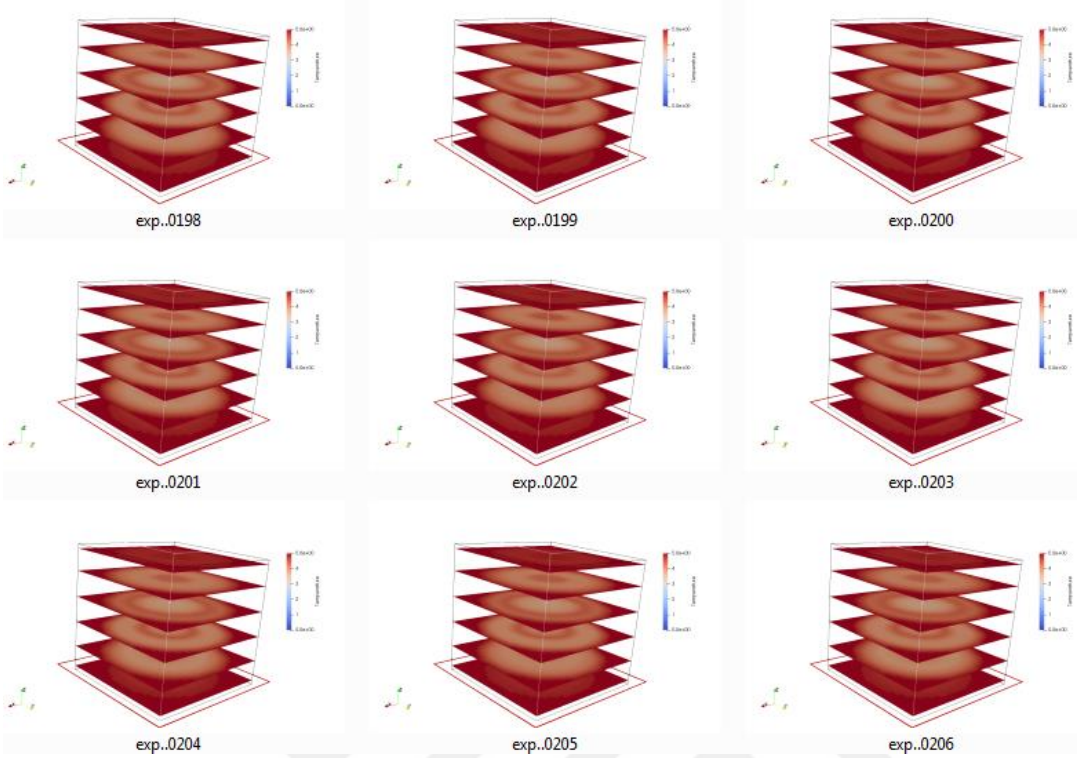

Figure A.23. Time steps of 198-206

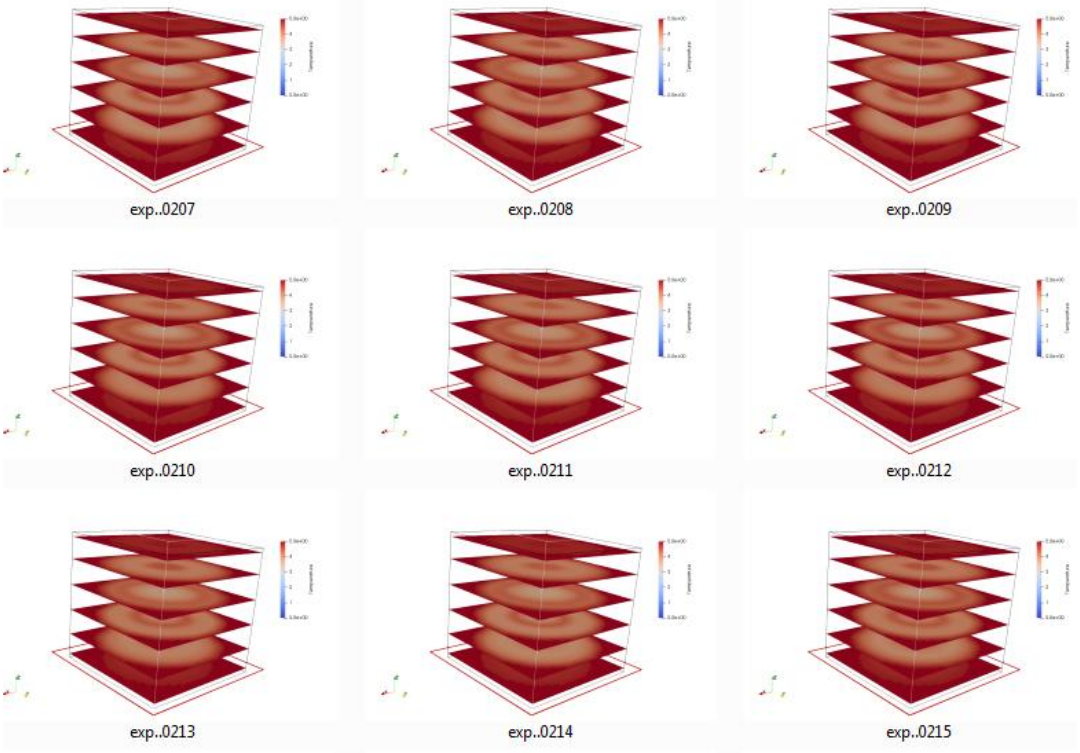

Figure A.24. Time steps of 207-215

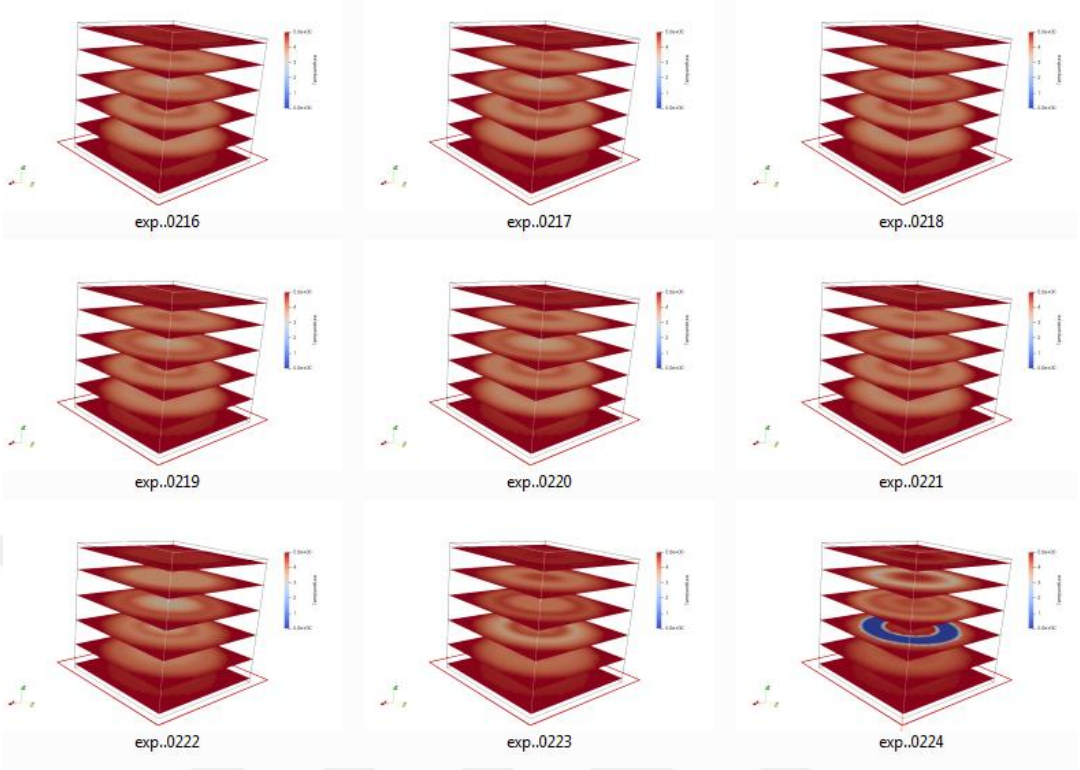

Figure A.25. Time steps of 216-224

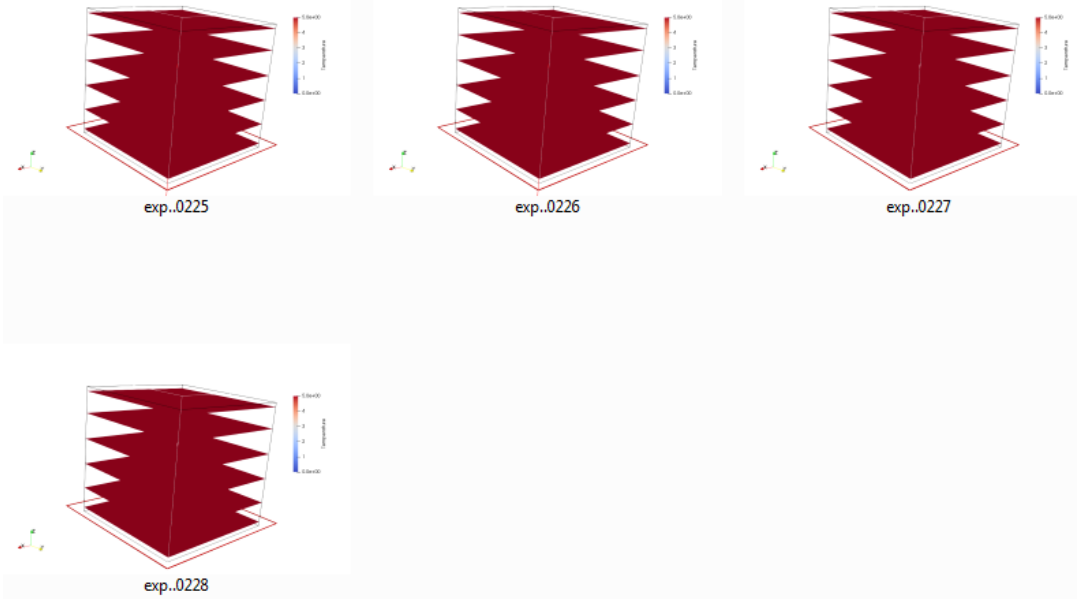

Figure A.26. Time steps of 225-228